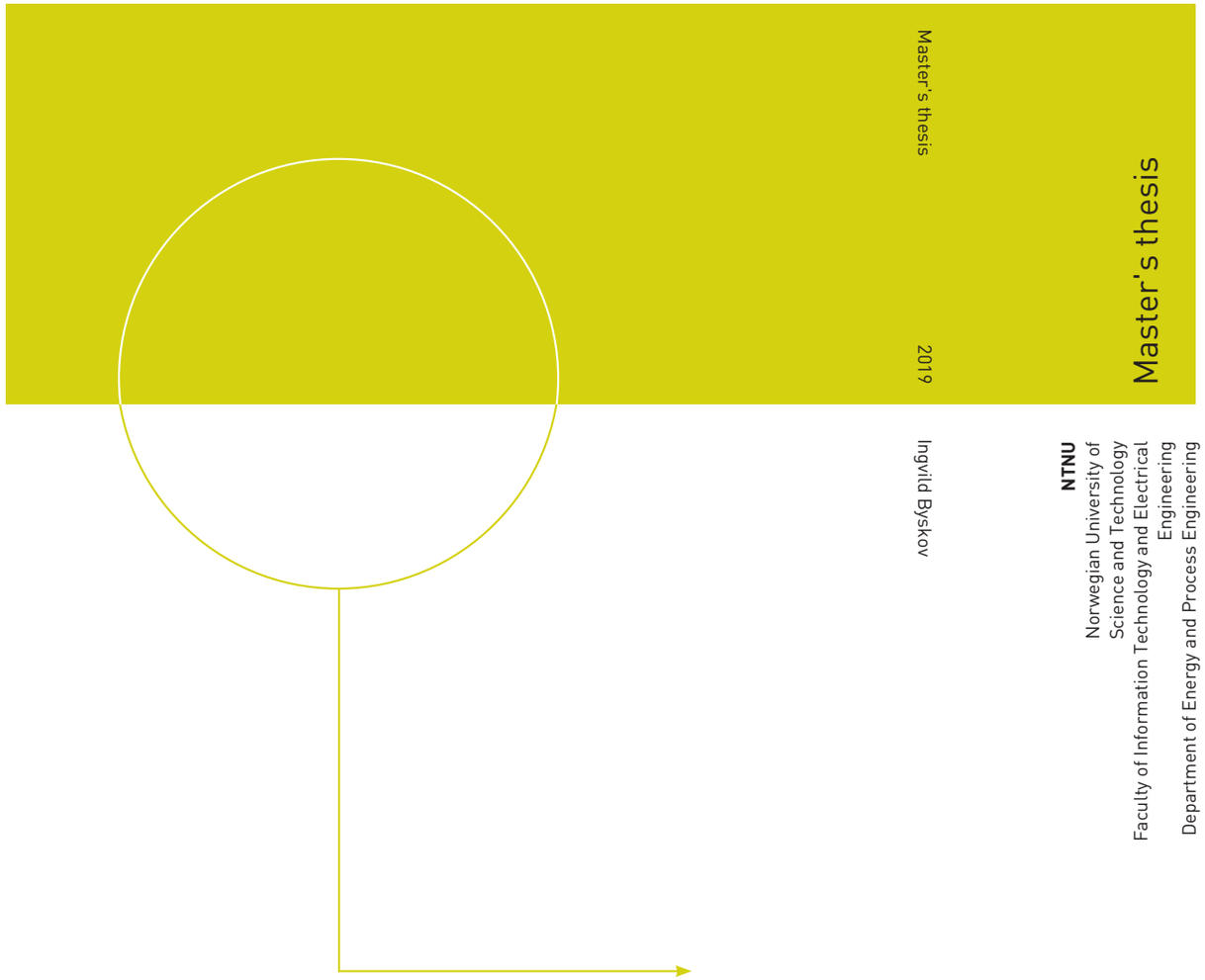

Master's thesis

2019

Ingvild Byskov

NTNU
Norwegian University of
Science and Technology
Faculty of Information Technology and Electrical
Engineering
Department of Energy and Process Engineering

Ingvild Byskov

Comparison of Recent Land-Use and Land-Cover Changes in Norway and the Tibetan Plateau

A spatiotemporal analysis based on satellite data from the ESA CCI-LC maps from 1992 to 2015

July 2019

NTNU
Norwegian University of
Science and Technology

NTNU
Norwegian University of
Science and Technology

NTNU

Norwegian University of
Science and Technology

Comparison of Recent Land-Use and Land-Cover Changes in Norway and the Tibetan Plateau

A spatiotemporal analysis based on satellite data from the ESA CCI-LC maps from 1992 to 2015

Ingvild Byskov

Energy and Environmental Technology
Submission date: July 2019
Supervisor: Francesco Cherubini
Co-supervisor: Jan Sandstad Næss, Xiangping Hu

Norwegian University of Science and Technology
Department of Energy and Process Engineering

Abstract

As humans grow in numbers, so does the associated ecological footprint. Anthropogenic Land-Use and Land-Cover Change (LUCC) has through time resulted in local and global impacts to the extent that there is nearly no place left on Earth that has not been influenced in some way. At current emission rates of 10-12 Gt CO2-eq per year, the aggregated sector of Agriculture, Forestry and Other Land Use are contributing to one fourth of total yearly anthropogenic Greenhouse Gas (GHG) emissions, and hence driving climate change. LUCC have the potential to impact, and be impacted by, the rate of climate change. The ways in which terrestrial ecosystems respond to stressors such as rising temperatures or different land use activities is poorly understood and there is a great great need for further research within this field.

With the recent global land cover maps from the European Space Agency (ESA) Climate Change Initiative (CCI), the CCI land cover (CCI-LC) project partly overcomes some of the characteristic challenges of land cover data, such as long-term consistency and spatial and temporal resolution. The most recent land cover product consists of long-term annual and consistent global maps at 300 m resolution. These land cover maps, from 1992 to 2015, were in this thesis used to study recent land cover changes in Norway and the Tibetan Plateau. A spatiotemporal data analysis, that consisted in mapping and computing trend lines for transitions of interest, revealed the revealed the biggest LUCC in the study areas.

Declining wetlands in Norway and greening in the Tibetan Plateau are the main characteristics for the studied time period. Both countries have conservation policies that aim to reduce the damage on important ecosystems, but these may still be at risk due to climate change and LUCC. Interactions between these need to be better understood in order to ensure effective policies in a changing climate. Improving and increasing the available data foundation through ground observation and integrated remote sensing systems, such as the CCI-LC maps, should play an important part in the race towards a sustainable future.

Sammendrag

I takt med en økende befolkning øker også det økologiske fotavtrykket. Menneskepåvirkede endringer i landareal og bruken av disse har over tid resultert i lokal og global påvirkning i den grad at det nesten ikke finnes steder på jorden som er uberørt av mennesker. Med dagens utslippsintensitet på 10-12 Gt CO2-eq per år bidrar jordbruk, skogbruk og annen arealbruk tilsammen med en fjerdedel av de totale årlige menneskeskapte drivhusgassutslippene, som igjen fører til klimaendringer. Endringer i landareal og -bruk har potensial til å påvirke, og bli påvirket av, klimaendringene. Måten landøkosystemer reagerer på ulike typer stress som stigende temperaturer eller landbruksaktiviteter er dårlig forstått og det er store behov for mer forskning og bedre data på området.

Med sine nyeste globale landkart fra European Space Agency (ESA) Climate Change Initiative (CCI), overkommer prosjektet for landdekke (CCI-LC) delvis noen av de utfordringene som kjennetegner slike data, for eksempel konsistens over tid og romlig og tidsmessig oppløsning. Det nyeste landdekkeproduktet består av langsiktige årlige og konsistente globale kart av 300 m oppløsning. Disse årlige landdekkskartene, fra 1992 til 2015, ble i denne oppgaven brukt til å studere nylige endringer i landdekke i Norge og Tibetplatået. Dataanalyse bestående av kartlegging og trend-analyse for overganger mellom ulike landklasser av interesse identifiserte de sentrale endringene i landdekke i studieområdene.

Reduksjon av våtmarkareal i Norge og greening i Tibetplatået er de viktigste observasjonene fra studieperioden. Begge landene har en aktiv naturforvaltning som tar sikte på å redusere de skadelige effektene på viktige økosystemer, men disse kan fortsatt være truet av klimaendringer og endringer i landdekke og endret landutnyttelse. Samspillet mellom disse ulike faktorene må forstås bedre for å sikre effektive reguleringer og politikk i et klima i endring. En forbedring av og økning i det tilgjengelige datagrunnlaget for landdekke, gjennom bakkeobservasjoner og integrerte fjernsansingssystemer, som de satellittbaserte CCI-LC-kartene, bør spille en viktig rolle i kappløpet for en bærekraftig fremtid.

Preface

This MSc thesis was performed during the last semester of the five year integrated Master Programme of Energy and Environmental Technology at the Norwegian University of Science and Technology (NTNU) in Trondheim, spring 2019. It is the final work of my Masters specialization in Energy and Environmental Analysis.

I am truly grateful for the supervision and guidance provided to me by my supervisor Francesco Cherubini, Professor and Director of the Industrial Ecology Programme at NTNU. Accompanied also by two highly skilled and kind co-supervisors from the same programme, PhD candidate Jan Sandstad Næss and Senior Researcher Xiangping Hu, you have all contributed to make the thesis work a valuable and fun learning process. A big thank you for your critical and positive insights, quick responses and continuous encouragement from beginning to end.

Contents

List of Figures

List of Tables

LIST OF ABBREVIATIONS

AVHRR	Advanced Very High Resolution Radiometer
CCI	Climate Change Initiative
CCI-LC	Climate Change Initiative Land Cover
ESA	European Space Agency
FAO	Food and Agriculture Organization of the United Nations
GHG	Greenhouse Gas
IDV	Integrated Data Viewer
IPCC	Intergovernmental Panel on Climate Change
LC	Land Cover
LCCS	Land Cover Classification System
LUCC	Land-Use and Land-Cover Change
MERIS	Medium Resolution Imaging Spectrometer
MITISTRESS	Strategies to Mitigate Pressures on Terrestrial Ecosystems from Multiple Stressors
PFT	Plant Functional Types
PROBA-V	Project for On-Board Autonomy; V stands for Vegetation
SPOT-VGT	Satellite Pour l'Observation de la Terre; VGT stands for Vegetation
UN	United Nations

1 Introduction

1.1 Background and motivation

1.1.1 Land use and land cover change in a climate context

Hardly any place on Earth remains unaffected by human activity [1], and it is therefore crucial to understand how different ecosystems are impacted, directly or indirectly, by anthropogenic drivers. Land use change and related activities emit approximately 4.3-5.5 Gt CO2-eq/yr [2]. Adding agriculture and forestry makes the yearly total 10-12 Gt CO2-eq, which corresponds to about 25 % of the yearly total of anthropogenic Greenhouse Gas (GHG) emissions [2]. Certain types of Land Cover (LC) such as wetlands, peatlands and permafrost represents a crucial role in climate change mitigation through conservation and restoration due to their high carbon content [2]. There is large uncertainty linked to the estimates of the potential emissions of degradation of these ecosystems [2], but studies suggest that in a future with climate change one of the largest positive (i.e., reinforcing) climate feedback mechanisms will be the thawing permafrost [3].

Understanding how Land-Use and Land-Cover Change (LUCC) affect the climate is complex, due to the variation of spatially and time dependent parameters. According to the Food and Agriculture Organization of the United Nations (FAO), LC can be described by the composition of natural, modified and artificial systems occupying the Earth's land surfaces, also reflecting all land based processes [4]. In contrast to land use, LC is a more concrete measurement that provides easy detection of anthropogenic land use [4]. Such data is important for climate change analysis and the study of carbon stocks and dynamics, and other natural phenomena [4]. The analyses are useful in different types of management such as land use planning and monitoring agricultural development, and crucial for the successful implementation of various programs within food security and other humanitarian and environmental causes [4].

Changes in vegetation can be caused both by anthropogenic activities and climate change [5], and it may be challenging to separate these factors. There is a need for a better understanding on how vegetation cover is altered by drivers such as climate change, CO2 fertilization effects, nitrogen deposition and land cover change [6]. Furthermore, changes in land and vegetation cover may in turn affect the climate through changes in the Earth's surface energy balance [7]. Figure 1 illustrates very simplified how terrestrial biomes and other factors are interconnected, and hence need to be researched and approached in a systemic manner to ensure effective environmental and climate policies.

Recent studies [6, 9] show that most of the Earth is greening, and the opposite effect that is browning, is observed in relatively few areas. "Greening and browning are defined as statistically significant increases and decreases, respectively, in the annual average green leaf area at a location over a period of several years" [9]. On a global level, as found in a study observing changes in leaf area from 1982 to 2009 [6], the main cause for recent greening seem to be an increase in gross primary productivity and CO2 fertilization effect. For the Tibetan Plateau and places located at northern high latitudes such as Scandinavia, greening trends can be explained largely by climate change foremost rising temperatures [6]. Both local plant growth and hydrology is vulnerable to changes in surface temperature, and especially critical effects may be related to temperature impacts on thawing and permafrost [10].

In recent decades there have been an extraordinary development in the availability of advanced technologies and scientific knowledge on the state of the Earth systems. Two factors that have been of significant importance for the development in land mapping are digitalization and the addition of new earth observation satellites [4]. This have made it easier to better integrate and interpret the data and as such improve the comprehension of the character and magnitude of issues related to anthropogenic emissions and intervention caused by the increasing industrialization and urbanization of the World. However, the utility of satellite observations are still limited and highly connected with uncertainty, especially in regions located at high latitudes with a mountainous topography due to weather and sun conditions (among others), that make remote sensing technologies challenging [11]. The importance of improving the quality of LC data is furthermore highlighted by the potential benefits this would offer in terms of food planning, net carbon balance estimation and conservation prioritization for critical ecosystems such as wetlands [12].

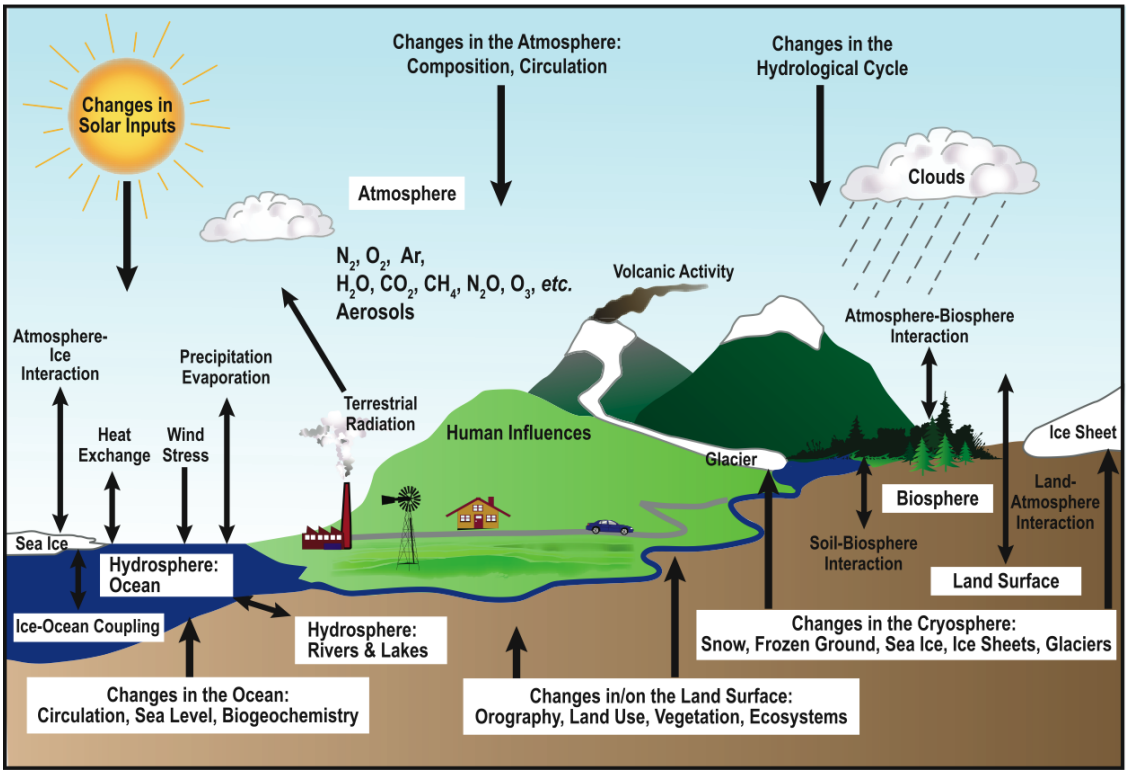

Figure 1. Natural and anthropogenic interactions relevant for the understanding of stressors on terrestrial ecosystems [8]

Besides satellite observations, there is also a great need for increasing the existing database from field studies that can validate vegetation data for vegetation-climate models [11]. However, as opposed to data collection based on field observations, remote sensing systems offer the benefit of global and regional imagery independent on where field work or measurement stations are situated. This is an important aspect of consideration when studying area of complex terrain such as the Tibetan Plateau [10]. Satellite data is also the only applicable information source for global dynamic vegetation and land surface models based on vegetation cover maps [13]. However, a continuous challenge in the field of LUCC is the acquisition of high quality data of sufficient spatial and temporal resolution [14], an issue that the European Space Agency (ESA) Climate Change Initiative Land Cover (CCI-LC) project is contributing to overcome. What is unique about the new products from Phase 2 of the Climate Change Initiative (CCI) is the high level of detail and temporal extent of the LC maps; long-term time series (1992-2015) at 300 m spatial resolution that are consistent with the United Nations (UN) Land Cover Classification System (LCCS). Although the data does not serve as direct input to climate models, the standardized classification scheme and provided conversion tables facilitate the use in modelling applications [15, 16]. As such, the CCI-LC maps may serve as the principal data foundation for a variety of climate models and land surface models to quantify LC interactions with the atmosphere and analyse recent carbon dynamics [13].

1.1.2 Regions of study

The Tibetan Plateau

Commonly referred to as the "Roof of the World", the "Third Pole" or the "Water Tower of Asia" the Tibetan Plateau is of high interest for climate change science [17, 18], both due to its importance for several ecosystem and climate regulatory services and because it is a sparsely populated area [5]. The latter makes it easier to distinguish between impacts caused by human activities and those caused by climate change.

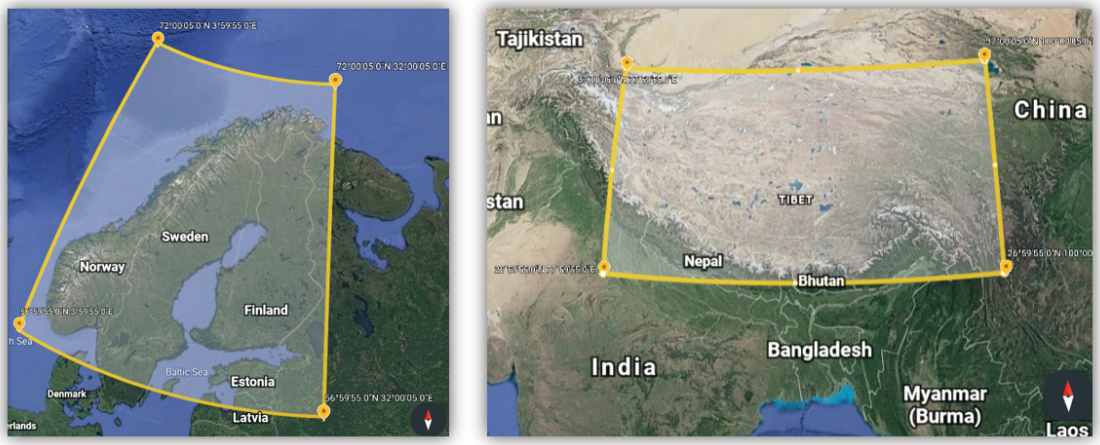

Figure 2. Scandinavia and Tibet area cut for this study. Mapped with Google Earth (`https://www.google.com/earth/`)

The Plateau has an average elevation of more than 4,000 meters above sea level [19], and is identified as an area highly sensitive and fragile to climate change perturbations [19, 20, 21]. Furthermore it is a region with significant potential to affect the climate both on a regional and global level; globally by impacting the Northern Hemisphere atmospheric circulation through the occurrence of LC changes [10]. The atmospheric, hydrological, environmental, geological and cryospheric conditions and processes at the Plateau affect biodiversity, water cycles and the climate on the planet [21]. The topographically complex character of the Tibetan Plateau makes it difficult for climate models to provide reliable predictions of future LC changes in the area [21]. This is moreover problematic for the population depending on the rivers that originate from this region [10]. The continuous runoff from major rivers such as the Yellow River, Yangtze River, Mekong River, and Salween River may change as a result of alterations in local land surface and climate conditions [10], putting people at risk of getting cut off from their lifeline. As much as 40 % of the world population are influenced by, or dependent on, these water sources [22].

Grassland is the dominating LC class at the Tibetan Plateau (Figure 3) and represents a crucial grazing ecosystem [22]. Vegetation is spatially distributed more intensively to the southeast of the Plateau, and decrease as you move towards the northwest, an area more characterized by desert landscape, correlating with precipitation patterns in the region [10]. In addition to great spatial variability, rainfall in the Tibetan Plateau is also characterized by being unevenly distributed in time, with 60 % of annual precipitation occurring during summer [10]. In regards to change patterns, a reinforcing effect has been observed for the last decades (1961-2005) in terms of more rain in the southeast regions and less rain in the drier northwest areas [10].

Three main national policies have lead to a significant recent shift in settlement and land use over the Tibetan Plateau, namely the "Grain to Green" policy, the "Ecological Migration" and the education law that is currently used in a bigger extent against herders that to not comply with the requirement of nine years of schooling [22]. Due to the vital importance of Tibetan grasslands, the Grain to Green policy (initiated in 1999), also referred to as "Rangeland to Grassland" where grasslands represent the main ecosystem, set out to save degraded grasslands by relocating herders from their grazing-based farms to a more livestock-based living in the urbanized east of the Plateau [22]. To avoid further overgrazing and protect the environment around the important head-waters and rivers of the region, the Ecological Migration policy pushed further traditional herders to urban areas [22].

5.1 billion people have socioeconomic interests in and around the Tibetan Plateau related to resources such as pasture and timber, and opportunities the area offers in terms of tourism and recreational activities [21]. A great number of people may therefore potentially be affected by changes in the sensitive ecosystems of the Tibetan Plateau. All of these considerations elucidate the region's important role not only for local and regional sustainability, but also for the global population and environment. Since change issues at the

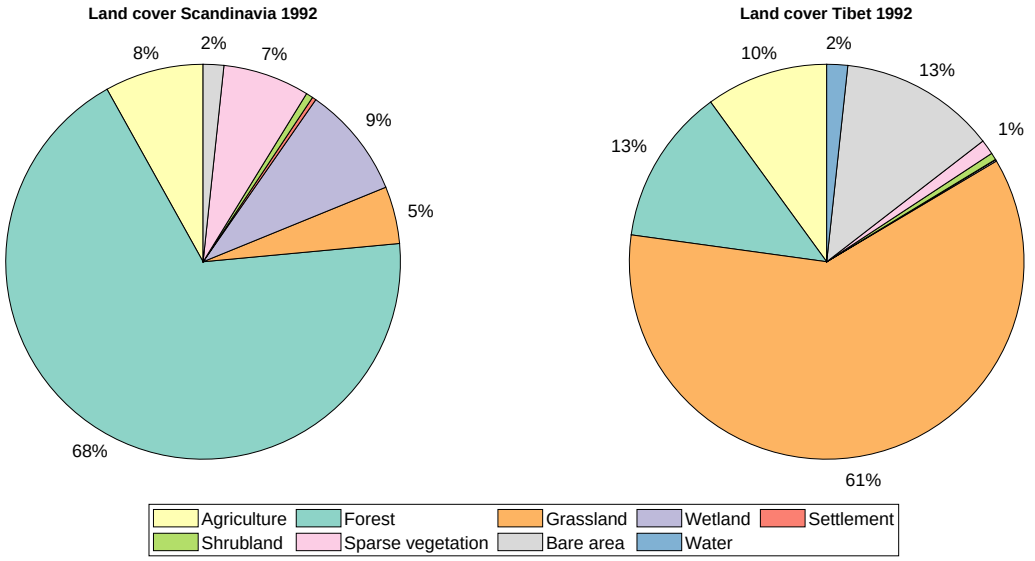

Figure 3. Area shares for the different LC categories (as classified by the IPCC in % of total land area, based on data from the CCI-LC map for 1992. LC classes with area fractions less than 1 % are not shown with numbers. Note that "Water" is excluded for Scandinavia, to avoid counting ocean water as a part of total land cover.

Plateau may both have global effects as well as global causes, it is crucial that the international community is engaged in collective efforts to improve the data foundation, that is currently of too low quality to provide accurate measures on the environmental, societal and economic linkages to changes in the dynamic nature of the Plateau, needed to initiate effective strategies for adaptation and mitigation [21].

Norway

Forming part of the Scandes mountain range from north to south [11], mainland Norway (without Svalbard and Jan Mayen) is 32.38 million hectares, of which about 30.41 million hectares (93.9 %) are land cover and 1.97 million hectares (6.1 %) freshwater bodies [23]. This mountainous country has elevations ranging from sea level to 2469 meters above sea level as the highest point [11]. It has a long Atlantic coastline to the west, and the terrestrial neighboring countries to the east are Sweden, Finland and Russia.

Forest has the major terrestrial LC share in Norway (Figure 3). Historically, forest resources has been exploited for timber and moved way for agriculture and other land use. When halted, this long lasting deforestation has opened up for natural tree regrowth [24]. This questions whether the recent forest growth in Norway is caused by historical human land use activities (and the subsequent regrowth potential) or anthropogenic driven climate change [24]. However the forestry sector still occupies large land areas in Norway, whereas eastern and central Norway has the largest share of the industry [25]. Despite that recent forest regulations take on a more environmental and conservation oriented approach [26], historic land use activities related to the forestry industry may have had serious impacts on other natural ecosystems such as wetlands. Drainage, logging and construction of infrastructure are some of the major influencing factors [27]. There are however national and international conservation plans and initiatives to protect threatened biodiversity and mitigate future release of GHG arising from the degradation of wetlands [28]. Although there may be uncertainties in the exact effect of the restoration of degraded wetlands, such efforts are considered to be some one of the most cost efficient mitigation options that exists today [29].

Norwegian lands have also been influenced by agricultural development, which shares the European tendencies of intensification [30, 31]. Farming has largely been moved away from remote and less fertile lands in favor of more centralized locations with fertile soils [32]. Compared to many other European countries, Norway has experienced this agricultural intensification to a lesser degree, due to challenging topography

and climate conditions in combination with regional politics to sustain marginal farming communities [30]. Mountain areas have been especially affected by the agricultural shift [32], and in Norway it has lead to a forest expansion in the subalpine zone [31].

1.2 Problem description

A valuable indicator for assessing the state of global change issues such as climate change is the long-term change in land cover and land use. In a time when it is crucial to adapt to a changing climate as well as mitigate further changes and improve food security, mapping and analysing land cover changes may provide essential contributions to understanding the impacts from climate change and reducing its related uncertainty, as well as guiding national policies for land use management.

The recent satellite-based global LC maps from the ESA CCI offer with its long-term annual time series and high spatial accuracy an important application and contribution to LUCC science and to the climate modeling community. The work of this master thesis will revolve around studying CCI-LC data for two areas, namely Norway and the Tibetan Plateau, and analyse the major LC changes that occurred in the data period i.e., 1992-2015. By exploring the recent historical land cover changes through data analysis, possible correlations with land use and climate change will be discussed. The work is linked to the recently initiated research project Strategies to Mitigate Pressures on Terrestrial Ecosystems from Multiple Stressors (MITISTRESS), a collaborative project between the Norwegian University of Science and Technology (NTNU), the Chinese Academy of Sciences and Beijing Normal University.

1.2.1 Research questions

With the above stated motivation, the thesis aims to answer two main research questions:

1. What are the major land cover changes of recent history in Norway and the Tibetan Plateau?
2. How can these changes be explained by different drivers?

Using the ESA CCI-LC this thesis seeks to quantify and identify major LC changes of recent character and present these in an intuitive and relevant manner to the formulated research questions. A trend (temporal) analysis and a spatial distribution analysis is performed to identify hot spots and gain a better understanding of LUCC based on where and when these have occurred.

1.3 Structure

The thesis follows a logical structure based on the IMRaD model: Introduction, Methods, Results and Discussion. Following the introduction of topic and study regions is a description of the applied methodology, which consists of an explanation of the data foundation, preparation and analysis. The latter is further divided into the three chosen analytical approaches, namely an initial analysis of all the gross and net transitions for both regions, followed by spatial and temporal analysis of selected transitions. Thereafter, the results are displayed in an identical sequence, and interpretation and discussion of these follow next. Aspects of uncertainty and ideas for further work will then be presented with some concluding remarks.

2 Methods

2.1 CCI-LC global annual maps

The original ESA CCI-LC data products, that provide the foundation of the data analysis, with user guide and tools are accessible at `http://maps.elie.ucl.ac.be/CCI/viewer/`. The user friendly and highly interactive web interface was created mainly for visualization purposes, as a space efficient alternative to

downloading the data sets when this is not necessary [15]. A screenshot of the main page can be seen in Figure 4.

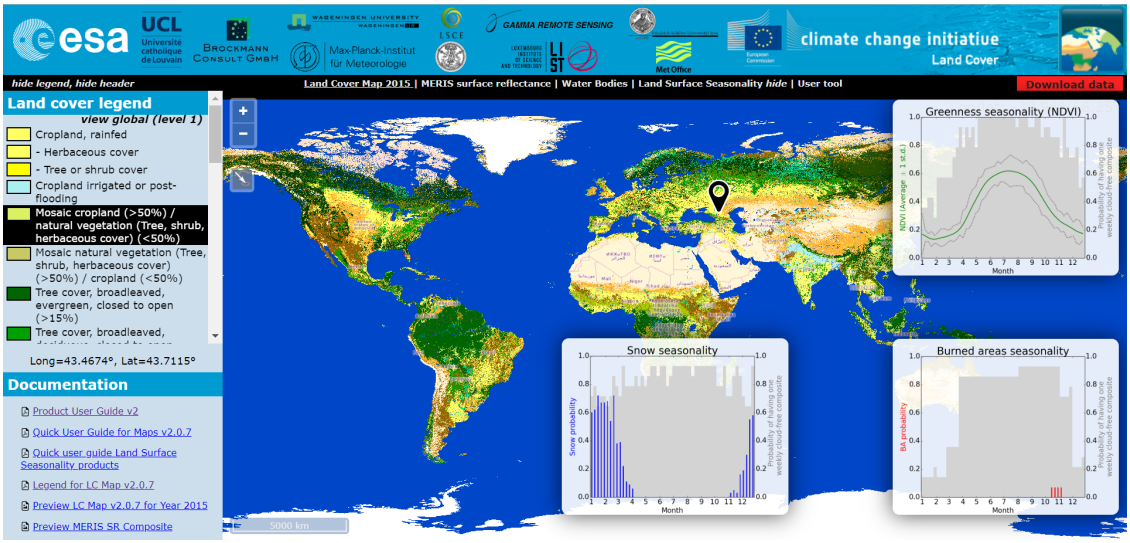

Figure 4. Main page of the web interface for the CCI-LC products

The analysis performed in this thesis is based on the global annual LC maps product, with coverage from 1992 up to and including 2015. The LC products are delivered as global files, with equirectangular (Plate Carrée) original projection and 300 m spatial resolution. The data is gathered from four different remotely sensed (satellite) products, namely the Advanced Very High Resolution Radiometer (AVHRR), SPOT-VGT, Medium Resolution Imaging Spectrometer (MERIS) (in full resolution (FR) at 300 m and reduced resolution (RR) at 1000 m), PROBA-V and corresponding metadata [15]. Possibilities for adjustments in projection and spatial resolution are offered by the CCI-LC user tool, and described in further detail in the User Guide [15]. In short, the tool consists of a conversion tool, aggregation tool and subset tool, all provided in order to prepare data for modelling purposes. Further specifications on the CCI-LC products and data sources is provided in appendix A. The ESA evaluates the overall accuracy of its CCI-LC maps to be about 71 %, but varying among the different LC classes and regions [15].

2.2 Study area

With motivation rooted in the MITISTRESS project, that aims to explore the impacts from stressors mainly related to LUCC in Norway and the Tibetan Plateau of China [8], a rough approximation of these geographical study areas was made; a "rectangle" map area was cut for each "region" (see Figure 2, Figure 6 and Figure 7), as it would be more complex and time consuming to cut out the actual shape of Norway and the Tibetan Plateau. For convenience, the areas of study are referred to as Tibet and Scandinavia throughout the thesis and when referring to the total area of each of these regions the term AREA CUT will be used. The inclusion of data from neighboring area naturally affects the results and its implications is discussed further in subsection 4.2.

Table 1. Coordinates (in decimal degrees) and total area of the selected area cut

Region	Latitude range	Longitude range	Total area (million ha)
Scandinavia	57.0 - 72.0	4.0 - 32.0	223.07
Tibet	27.0 - 37.0	78.0 - 100.0	230.52

Location data for the chosen Scandinavian and Tibet region is summarized in Table 1. The cut was made

as to include the entire mainland country of Norway (excluding Svalbard and Jan Mayen) and the entire Tibetan Plateau for "Scandinavia" and "Tibet", respectively. The former encompasses Norway, Finland, Estonia, most of Sweden, and parts of Denmark, Russia and Latvia. The latter includes in addition to the Tibetan Plateau in China, parts of the surrounding countries India, Nepal, Bhutan and Myanmar. In reality, the Tibetan Plateau stretches over the Tibetan Autonomous Region and the Chinese provinces of Yunnan, Sichuan, Qinghai, Gansu, and Xinjiang, as well as being partly situated in India, Nepal, Pakistan and Tajikistan [10].

2.3 Classification system

Due to the spectre of methodologies and data sources that exist for analyzing LC, comparison of different data sets may be challenging and hence affect the utility [4] and increase overall uncertainty. The lack of a globally accepted classification standard also prevent scaling up studies for e.g., cross-region applications [33]. Although limited, efforts are being made for improving LC data quality such as level of accuracy and consistency [4], and the CCI-LC maps have a legend that is based on such efforts, namely the standardized LCCS methodology defined by the UN FAO. The system can be used for mapping applications of a variety of scales and methodologies [33] and categorizes LC hierarchically into global classes ("level 1 legend") and regional classes ("level 2 legend") [15] (see Table 2). The level 2 legend contains region specific information, where available, and adds more detail to the global LC classes. The LCCS is designed to be applicable for a variety of LC analyses, so using this classification system facilitates the conversion between the CCI-LC classes and categories used in the environmental modeling community, such as the Plant Functional Types (PFT), which has its own look-up table in the LC CCI User Guide [15]. However, a more general classification system containing the main LC classes (e.g. forest) is highly preferred for climate modelling purposes due to the limitations and uncertainty arising from the application of PFT-maps converted from data sets of different epochs (which is the case for the CCI-LC products), which has the undesirable effect of underestimating LC change [34].

The Intergovernmental Panel on Climate Change (IPCC)-defined set of LC classes is an example of such a classification system and is also what is applied in this thesis; Table 3 shows the categorical conversion that was utilized for the aggregation from the CCI-LC legend. The IPCC categorization does not consider permanent snow and ice cover, so this is not covered in this analysis either.

The change detection is also only performed at the accuracy level of IPCC LC categories, although the original annual LC maps are given in LCCS labeled classes. This implies that transitions between LC classes belonging to the same IPCC category are not captured in the CCI-LC maps [15]. Furthermore, the change detection algorithm is based on 1 km observations, but delineated at 300 m to provide the higher resolution [15], meaning that only LC changes that can be identified from a distance of 1 km are detected. Lastly, it is dependent on observing a LC change over two consecutive years minimum in order to register the change.

2.4 Data preparation

The data foundation used in this thesis is from ESA CCI-LC gridded data sets, as shown in Figure 6 and Figure 7. These map cuts provided the starting point for the thesis work and were prepared as structured MAT-files containing the matrices of interest i.e., data on LC classes and area, LC change (transition fractions), and latitude and longitude data for each pixel (grid) element. Table 4 presents an overview of the data and the flowchart in Figure 5 illustrates the overall data procedure.

The original data can be directly downloaded as CSV-files from `http://maps.elie.ucl.ac.be/CCI/viewer/`. The raw data have the original spatial resolution of 300 m and are represented with pixel values corresponding to the UN LCCS classes presented in Table 2.

First, the aggregated data was studied. This consisted of matrices with fractional transition data that were already aggregated 18 times relative to the original resolution (in order to be less space consuming), as shown with matrix dimensions in Table 4. Fractional transitions here means that each element (pixel) in

Table 2. The LCCS-based legend used for the ESA CCI land cover maps [15], available from `http://maps.elie.ucl.ac.be/CCI/viewer/`. Values belonging to the global and regional legend are positioned towards the left and right margins, respectively.

Value	Label	Color
0	No Data	
10	Cropland, rainfed	
11	Herbaceous cover	
12	Tree or shrub cover	
20	Cropland, irrigated or post-flooding	
30	Mosaic cropland (>50%) / natural vegetation (tree, shrub, herbaceous cover) (<50%)	
40	Mosaic natural vegetation (tree, shrub, herbaceous cover) (>50%) / cropland (<50%)	
50	Tree cover, broadleaved, evergreen, closed to open (>15%)	
60	Tree cover, broadleaved, deciduous, closed to open (>15%)	
61	Tree cover, broadleaved, deciduous, closed (>40%)	
62	Tree cover, broadleaved, deciduous, open (15-40%)	
70	Tree cover, needleleaved, evergreen, closed to open (>15%)	
71	Tree cover, needleleaved, evergreen, closed (>40%)	
72	Tree cover, needleleaved, evergreen, open (15-40%)	
80	Tree cover, needleleaved, deciduous, closed to open (>15%)	
81	Tree cover, needleleaved, deciduous, closed (>40%)	
82	Tree cover, needleleaved, deciduous, open (15-40%)	
90	Tree cover, mixed leaf type (broadleaved and needleleaved)	
100	Mosaic tree and shrub (>50%) / herbaceous cover (<50%)	
110	Mosaic herbaceous cover (>50%) / tree and shrub (<50%)	
120	Shrubland	
121	Evergreen shrubland	
122	Deciduous shrubland	
130	Grassland	
140	Lichens and mosses	
150	Sparse vegetation (tree, shrub, herbaceous cover) (<15%)	
151	Sparse tree (<15%)	
152	Sparse shrub (<15%)	
153	Sparse herbaceous cover (<15%)	
160	Tree cover, flooded, fresh or brakish water	
170	Tree cover, flooded, saline water	
180	Shrub or herbaceous cover, flooded, fresh/saline/brakish water	
190	Urban areas	
200	Bare areas	
201	Consolidated bare areas	
202	Unconsolidated bare areas	
210	Water bodies	
220	Permanent snow and ice	

each of the given transition (land cover change) matrices had the value of how much area had transitioned from one category (e.g. agriculture) to another (e.g. forest) relative to the total pixel area of that element. Since these matrices contained gross transitions from 1992 to 2015 (not with yearly data of intermediate transitions), there were eight two-dimensional transition matrices for each of the nine LC categories i.e., 72 for each region and 144 in total. However, this data could not be utilized directly for further analysis before it was multiplied element-wise with its corresponding pixel area in order to get the absolute (not the relative) area change. Since there are differences in "real" pixel area as you move from one latitude (of

Table 3. Correspondence between the IPCC land categories and the legend used in the ESA CCI-LC maps [15]

IPCC Classes considered for the change detection		LCCS legend used in the CCI-LC maps	
1. Agriculture		10, 11, 12	Rainfed cropland
		20	Irrigated cropland
		30	Mosaic cropland (>50%) / natural vegetation (tree, shrub, herbaceous cover) (<50%)
		40	Mosaic natural vegetation (tree, shrub, herbaceous cover) (>50%) / cropland (< 50%)
2. Forest		50	Tree cover, broadleaved, evergreen, closed to open (>15%)
		60, 61, 62	Tree cover, broadleaved, deciduous, closed to open (> 15%)
		70, 71, 72	Tree cover, needleleaved, evergreen, closed to open (> 15%)
		80, 81, 82	Tree cover, needleleaved, deciduous, closed to open (> 15%)
		90	Tree cover, mixed leaf type (broadleaved and needleleaved)
		100	Mosaic tree and shrub (>50%) / herbaceous cover (< 50%)
		160	Tree cover, flooded, fresh or brakish water
		170	Tree cover, flooded, saline water
3. Grassland		110	Mosaic herbaceous cover (>50%) / tree and shrub (<50%)
		130	Grassland
4. Wetland		180	Shrub or herbaceous cover, flooded, fresh-saline or brakish water
5. Settlement		190	Urban
6. Other	Shrubland	120, 121, 122	Shrubland
	Sparse vegetation	140	Lichens and mosses
		150, 151, 152, 153	Sparse vegetation (tree, shrub, herbaceous cover)
	Bare area	200, 201, 202	Bare areas
	Water	210	Water

a satellite image) to another, especially at high latitudes, the area matrix used for the multiplication was already adjusted for this i.e. it contained the actual area of each element. After the multiplication, each transition matrix indicated how much of what was observed and characterized as e.g. "Agriculture" in 1992 transitioned to e.g. "Forest" in 2015.

Later on, the original (not aggregated) data from the CCI-LC maps was used to provide insight to the spatio-temporal dimension of the LC changes. This data consisted in 24 yearly matrices (1992-2015) for each region with pixel values corresponding to the LC classes in the specific year. As opposed to the computed and aggregated transition matrices, the set of original land cover matrices provided information on the spatial and temporal distribution of LC, allowing for a more detailed analysis. The downside of working with this data compared to the aggregated data set is the amount of time it takes to run through different computations element-wise. The following section describes the different utility of the two data sets.

2.5 Data analysis

All data analysis were performed in an equal manner for Scandinavia and Tibet. The aggregated transition matrices and the original LC matrices described in the above section were computed further in order to create different plots and tables for meaningful interpretation of the regional LC changes. Matlab was utilized for programming and plotting data, and Excel was also used for the latter. To visualize LC transitions in the spatial dimension, the map application Integrated Data Viewer (IDV) from Unidata was used.

Table 4. Dimensions of the provided area and land cover data. Here, "original" refers to the spatial resolution of the raw data (300 m), and "aggregated" refers to the data that was aggregated 18 times compared to the original.

		Matrix dimension	
Data type	Description	Scandinavia	Tibet
Area matrix, aggregated	Matrix containing actual pixel area data of the aggregated resolution (square kilometers)	560 x 300	440 x 200
Land cover change (transition) matrices, aggregated	Matrices with relative (to pixel area) gross transitions for each LC class (i.e., one matrix shows gross area change from one LC class to another LC class) based on land cover maps from 1992 and 2015	560 x 300	440 x 200
Latitude vector, aggregated	Vector containing latitude data of the area cut in aggregated resolution (decimal degrees)	300 x 1	200 x 1
Longitude vector, aggregated	Vector containing longitude data of the area cut in aggregated resolution (decimal degrees)	560 x 1	440 x 1
Area matrix, original	Matrix containing actual pixel area data (hectares)	10082 x 5402	7922 x 3602
Land cover matrices, original	Yearly matrices with original LCCS data (LC classes)	10082 x 5402	7922 x 3602
Latitude vector, original	Vector containing latitude data of the area cut (decimal degrees)	5402 x 1	3602 x 1
Longitude vector, original	Vector containing longitude data of the area cut (decimal degrees)	10082 x 1	7922 x 1

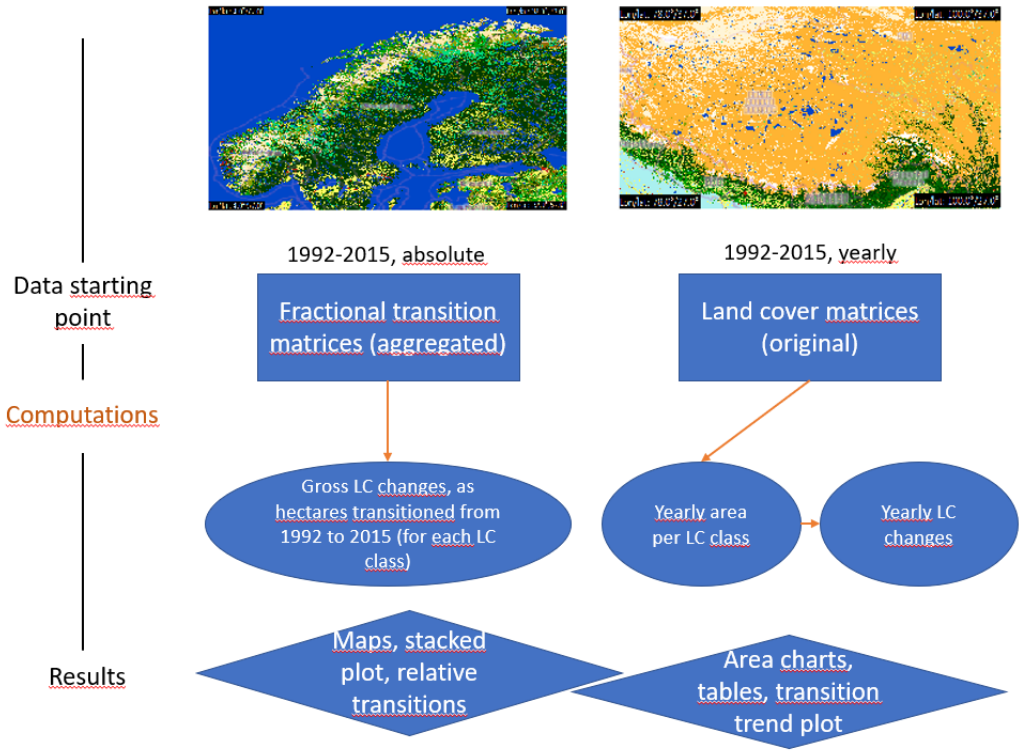

Figure 5. Simplified methodological approach

Figure 6. CCI-LC map from 2015 for the Scandinavia area cut [35]. Displayed with the original legend found in Table 2.

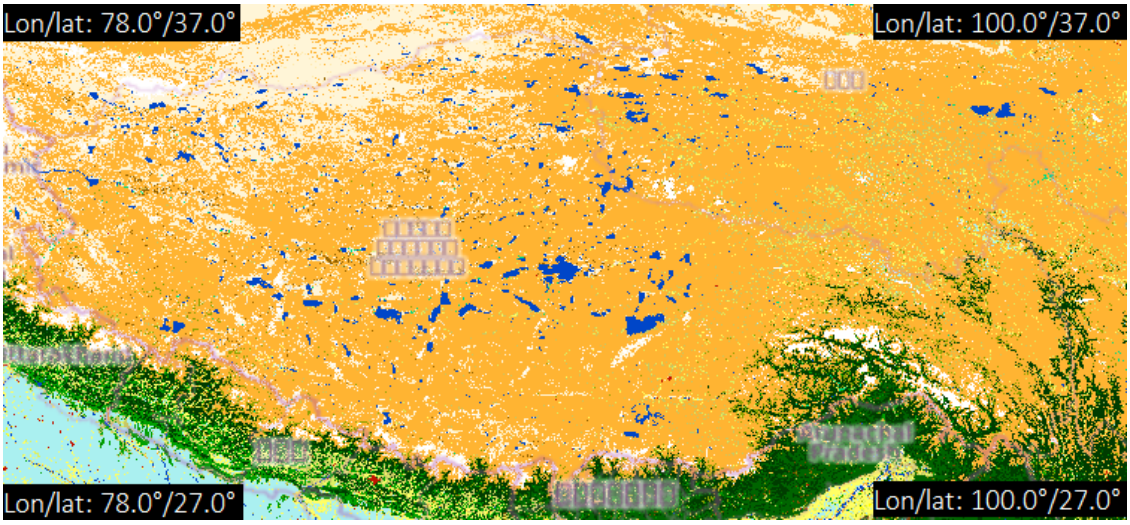

Figure 7. CCI-LC map from 2015 for the Tibet area cut [35]. Displayed with the original legend found in Table 2.

2.5.1 Calculation of gross and net land cover changes

Based on the aggregated transition matrices, a stacked bar chart (or mirror bar chart) was created for Scandinavia (Figure 9) and Tibet (Figure 10). This was made in Excel, with matrices generated in Matlab providing the input data for the charts; one 9-by-9 matrix for each region, with each element representing the total area (in hectares) of one specific transition e.g. agriculture to forest. For each LC class, the row elements contained its gross loss ("area transitioned from this class") to the different LC classes over the columns. Conversely, each column contained gross gains for the LC class in the specific column header. Each element was calculated by running through the aggregated transition matrices and adding every contribution for each transition into a total that was placed into this logical table structure (Table 9) that could be plotted. The net change (marked by a black circle in the figures) was calculated simply as the total area gained (summing the elements of the relevant column) minus total area lost (summing the elements of the relevant row), for each LC class.

Furthermore, the total area coverage of each LC class in 1992 and 2015 was calculated from the provided area matrix and land cover matrices of original resolution. This allowed for comparison between the LC changes on a relative basis i.e., how much of a certain LC type had transitioned to another between 1992-2015, relative to its own area coverage in 1992. The transitions were also calculated in shares of total (all LC classes) area, and presented in Table 5 as percentage gross loss and gain for each LC class. For Scandinavia, water is left out from these calculations and this table due to the methodological issue of counting ocean as part of the total water area in Scandinavia. So, when calculating total area of the area cut for Scandinavia, all water area is left out in order to avoid significant errors i.e., "total land area" that is the basis of the calculation of shares in the first of the two columns of the area loss and area gain, refers to the sum of all LC class area, except for water, in 1992. Although this implies that the inland water bodies of this region are not counted, it gives a less erroneous result than if including it. To provide an idea of how much freshwater surface area can be found in this study region, the total area of freshwater bodies in Norway represent 6 % of the area cover of mainland Norway [23]. Figure 2 shows that ocean is a significant bigger share of the water class for the area cut.

2.5.2 Spatial analysis

Spatial distribution analysis was performed with the Java-based visualization tool IDV from Unidata (in ongoing development at the Unidata Program Center in Boulder, Colorado) [36]. This software frame-

work can be downloaded free of cost via `https://www.unidata.ucar.edu/software/idv/docs/userguide/Starting.html` (IDV 5.6 desktop version was utilized for this thesis work). A software library and a reference application allow for visualizations of different geoscience data types and sources [36]. A comprehensive user guide is available at `https://www.unidata.ucar.edu/software/idv/docs/userguide/frames.html`.

The data inputs fed to the program were netCDF files, created in Matlab from the aggregated transition matrix and latitude and longitude vectors corresponding to each region of study (Table 4). Previous to being converted to netCDF files, the transition matrix was computed simply by extracting the fractional transition matrix of interest from the provided aggregated data set and perform element-wise multiplication with the aggregated area matrix. When imported to IDV, a map display based on the given data is created (see Figure 8), with each map pixel representing the corresponding matrix element containing the amount of area (in hectares) that changed from one LC class (in 1992) to another (in 2015, compared to 1992).

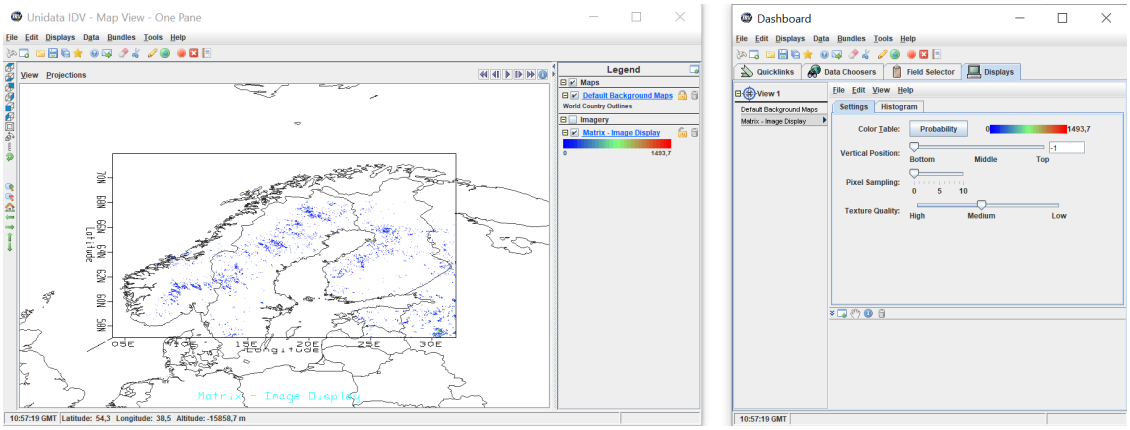

Figure 8. User interface of the IDV (Map Viewer to the left and Dashboard to the right)

The IDV map visualizations quantify the spatial distribution of gross LC changes between 1992 and 2015 by mapping each transition of interest individually. The maps are displayed with a legend (of colortable type "Probability") that indicates the intensity of change i.e., how many hectares of land transitioned in each colored pixel. In order to identify and emphasize hot spots, a "breakpoint value" is chosen for each transition type to separate the values above the breakpoint from the rest by marking these red (marks the high end of the scale). In order to allow for comparison between gross "mirror transitions" (e.g., "agriculture to forest" and "forest to agriculture"), these are assigned an identical breakpoint value (but may be different for Scandinavia and Tibet transitions). The change intensity need therefore be interpreted with this consideration in mind.

2.5.3 Time series analysis

In order to analyse how land was changing over the time period 1992-2015, quantitative information on the yearly LC distribution was needed. For both regions, 24 yearly area matrices for each LC class were calculated and structured into MAT-files (one for each LC class and region i.e., 18 in total) for further computation. To compute these area matrices, a Matlab code was created to run through the elements of the original yearly land cover matrices and recognize the LCCS classes that belonged to the IPCC LC class of interest using the conversion in Table 3, and subsequently identify the corresponding area (from the provided original area matrix) of this element in order to insert this into the new area matrix, hereby creating an area matrix containing only the area elements of the LC of interest and zeros in the other matrix cells. From these matrices, (total) area charts (e.g., Figure 32) could be easily generated by displaying the total yearly area found from summing all elements in the relevant matrix.

Another application of these area matrices was the creation of trend lines for specific transitions of interest (see Figure 41 and Figure 42). These were computed as yearly gross change from one class to another by comparing two years at a time, where the earliest year of the two (e.g. 1999) always belongs to the "from

class" and the subsequent year (2000) belonging to the "to class" of the specific transition of study. Running through the "from-matrix" and the "to-matrix" simultaneously, the Matlab code identified the values that were non-zero (e.g. contained the area of the LC classes of interest) at the same place in the matrix, and added these area elements into a vector that was used to create the trend plot.

3 Results

3.1 Gross and net land cover changes

By comparing gross and net land cover changes from 1992 to 2015 for each LC class (Figure 9 and Figure 10), the major transitions were identified for the Scandinavia and Tibet region. Table 9 in the appendix illustrates the transition matrix that was used to create these stacked bar charts, and contains all the numerical values of the gross transitions.

According to the IPCC-defined LC categories, Scandinavia experienced a net area increase of agriculture, grassland, settlement, shrubland and bare area. Forest, wetland, sparse vegetation and water showed to the contrary a net area loss throughout the 24-year mapping period. The LC transition that dominates in terms of net change in Scandinavia in the study period is the gain in agricultural land of 1.6 million hectares, equivalent to nearly 2.2 million soccer fields [37]. Grassland and settlement also show a significant net increase. Area changes in forest and sparse vegetation have contributed approximately equally to the growth in grassland, which is the LC class with the largest net increase after agriculture in Scandinavia. In terms of gross changes however, the dominating LC changes are found in the forest category, with the main transitions being from wetland to forest and forest loss to agriculture. Wetland has experienced the largest net area loss, a reduction of 1.7 million hectares since 1992.

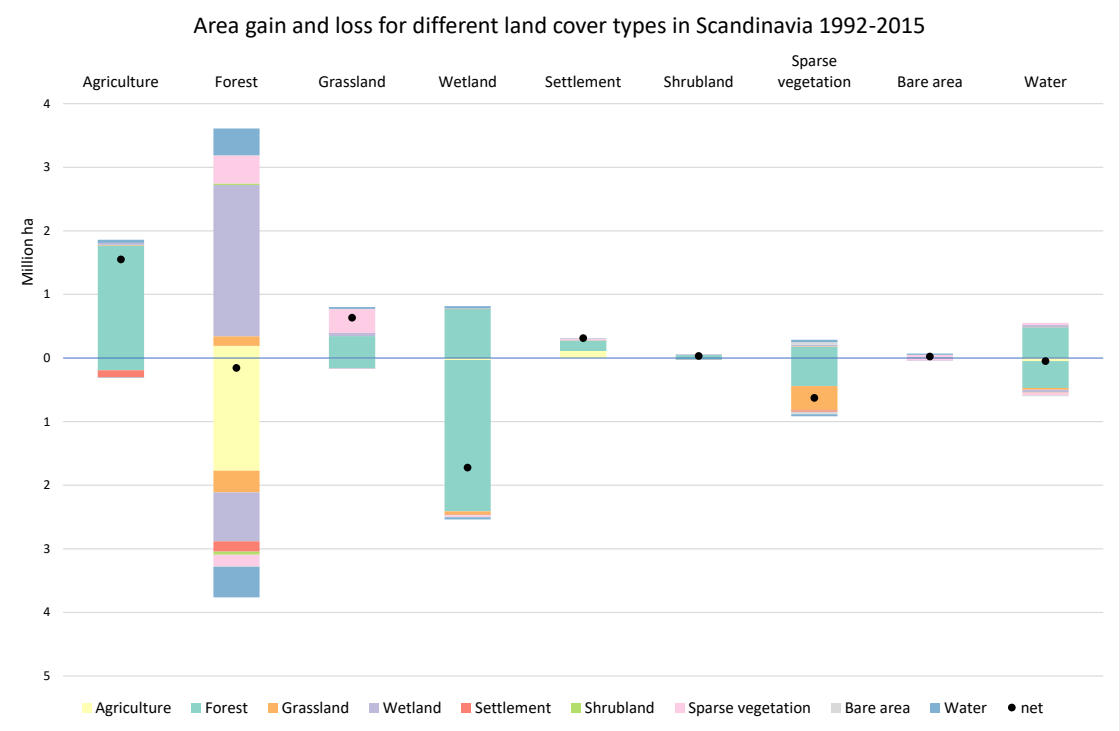

Figure 9. Land cover transitions for Scandinavia 1992-2015. Gross area gain for each LC class is represented by the bars above the horizontal axis, and gross area loss by the bars below the axis. Colors indicate between which LC classes the change has occurred e.g., "Wetland to Forest" is characterized by the purple-colored area of the forest column above the horizontal axis. The black dots mark net land cover change.

In the Tibet region, net gains were found for agriculture, forest, grassland, settlement, water and sparse vegetation. The latter experienced the greatest net gain among the LC classes, equal to 333 thousand hectares. The remaining LC categories wetland, shrubland and bare area show net losses over the study period. As forest was the most prevailing LC category for gross change in Scandinavia, grassland is standing out in Tibet, having the highest values both for gross loss and gain, and the second biggest net area gain (after sparse vegetation). 68 % of the gross increase in grassland comes from bare area, resulting in bare

area being the LC class with the biggest net decline, corresponding to a net loss of one million hectares over the study period. However, a significant amount of grassland has also been converted to bare area, namely 47 % of the grassland lost between 1992 and 2015.

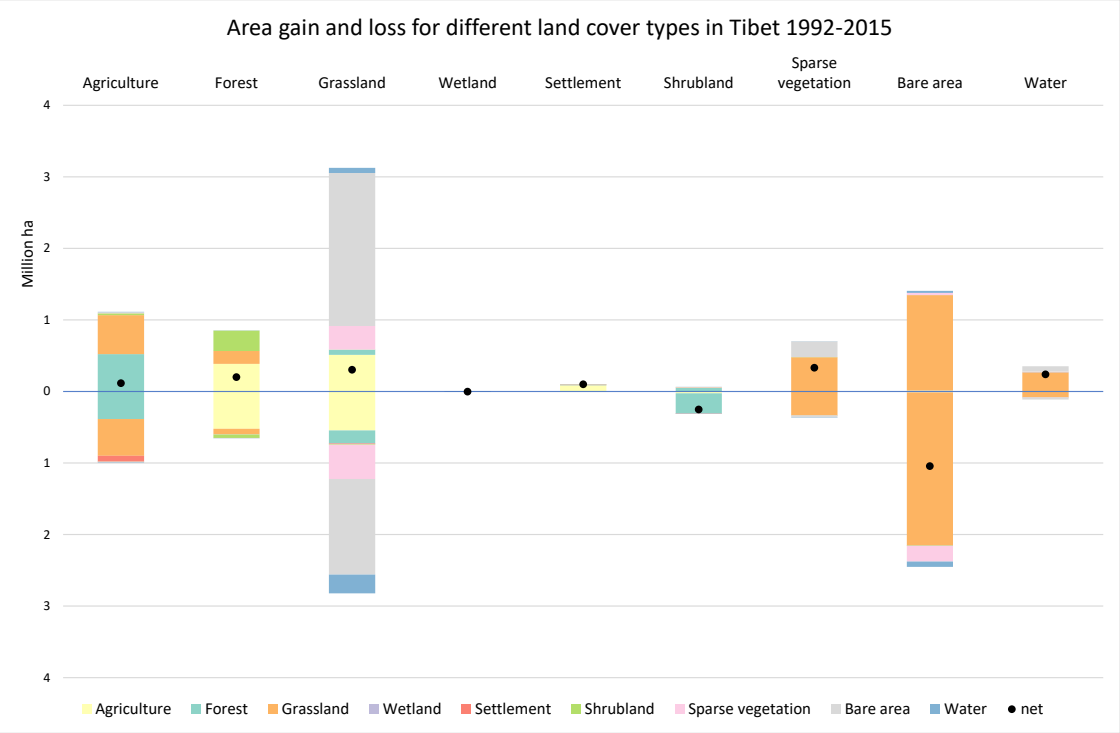

Figure 10. Land cover transitions for Tibet 1992-2015. Gross area gain for each LC class is represented by the bars above the horizontal axis, and gross area loss by the bars below the axis. Colors indicate between which LC classes the change has occurred and the black dots mark net land cover change.

Looking at agriculture, a clear difference between the two regions of study is that Scandinavia has seen a much stronger gross increase than loss i.e., there have been a significant growth of agricultural land in this area. Conversely, in Tibet the loss and gain tendencies in agriculture seem to mirror each other, also in terms of which type of LC changes are driving the gross increase and decrease. Grassland and forest represent the major contributions in terms of both area loss and gain of agriculture in Tibet. A similar "mirror effect" is also present among the grassland transitions in Tibet; despite the net gain of grassland in the region this gain is partially set back by grassland area lost mostly to LC classes identical to the ones that explain the grassland gains, that is bare area, agriculture, sparse vegetation, forest and water.

Based on the initial results visualized in the stacked bar charts (Figure 9 and Figure 10), nine gross LC changes for Scandinavia and ten for Tibet were identified as transitions of interest (major transitions):

- Scandinavia

  Agriculture $\Longleftrightarrow$ Forest

  Wetland $\Longleftrightarrow$ Forest

  Water $\Longleftrightarrow$ Forest

  Forest $\Longleftrightarrow$ Grassland

  Sparse vegetation $\Longrightarrow$ Grassland

- Tibet

  Bare area $\Longleftrightarrow$ Grassland

Grassland $\Longleftrightarrow$ Agriculture

Agriculture $\Longleftrightarrow$ Forest

Grassland $\Longleftrightarrow$ Sparse vegetation

Bare area $\Longrightarrow$ Sparse vegetation

Grassland $\Longrightarrow$ Water

These LC changes are the main focus of the spatial and temporal analysis to follow. The selection was made based on which LC classes contributed most to the observed area changes in the study period. The arrows indicate whether the transition was mapped for both of the gross changes (two-way arrow) or only for one of these (one-way arrow). The latter was chosen when only one of the "directions" was considered significant, such as "Sparse vegetation to Grassland" for Scandinavia. In order to understand LUCC and related drivers it is important to study the gross transitions (not only net); although the net change may be minimal, the gross changes may have have occurred at greatly different locations in space and time, and thus be a valuable indicator of local LUCC.

Furthermore, all transitions (except the ones related to water in Scandinavia) were also calculated on a relative basis i.e. computed as shares of each LC class' area in 1992 that had changed to another ("all other classes") when studied in 2015. The results of this calculation are displayed in Table 5. Water is left out for Scandinavia due to reasons explained in subsubsection 2.5.1.

The LC classes with the greatest absolute change values in the stacked bar charts are not necessarily the major ones on a relative basis. As Table 5 shows, this is especially the case for settlement, that in Scandinavia has increased by 80 % compared to 1992. This development is even more extensive in Tibet, that has experienced a gain in settlement area of almost 200 % since 1992. This is the only LC class that has developed exclusively in one direction i.e., that has no area loss (just gain) during the study period. Wetland is another LC class with substantial absolute and relative changes in Scandinavia; a net reduction of 15 % relative to 1992 wetland area is observed in this region. Both gross gain and loss almost exclusively originate from interchanges with forest area.

Table 5. Gross changes in land cover during 1992-2015 relative to land cover specific and total land area in 1992. Proportions of area changing from each LC class to 'all other' classes and from 'all other' classes to each LC class are shown in the columns for area loss and gain, respectively. As ocean area is counted within the water class (and not freshwater bodies solely), this category is excluded for Scandinavia.

Land cover class	Total area in 1992 (million ha)	Area loss		Area gain	
		% gross loss, relative to total land area	% gross loss, relative to LC area	% gross gain, relative to total land area	% gross gain, relative to LC area
Scandinavia					
Agriculture	9.95	0.25	3.12	1.51	18.69
Forest	84.09	3.06	4.48	2.93	4.29
Grassland	5.76	0.14	2.91	0.65	13.91
Wetland	11.27	2.06	22.51	0.66	7.24
Settlement	0.39	0.00	0.00	0.26	80.30
Shrubland	0.70	0.02	3.63	0.05	8.28
Sparse vegetation	8.73	0.74	10.48	0.23	3.28
Bare area	2.08	0.04	2.24	0.06	3.34
Water not considered					
Tibet					
Agriculture	22.52	0.44	4.44	0.50	4.95
Forest	28.83	0.29	2.26	0.38	2.96
Grassland	136.54	1.25	2.07	1.39	2.29
Wetland	0.29	0.00	2.00	0.00	1.59
Settlement	0.05	0.00	0.00	0.04	199.46
Shrubland	1.30	0.14	24.21	0.03	4.92
Sparse vegetation	2.75	0.16	13.33	0.31	25.43
Bare area	28.84	1.09	8.50	0.63	4.88
Water	3.85	0.05	2.94	0.16	9.16

3.2 Spatial analysis

Maps were generated in IDV for the major transitions listed in subsection 3.1 and the results from these visualizations quantify the spatial distribution of gross LC changes between 1992 and 2015. Since the color legend is scaled to a selected "breakpoint value" as explained in subsubsection 2.5.2, pixels of the same color intensity vary in magnitude across the maps. Hot spots are identified where there are pixel clusters and/or colors belonging to the high end of the color scale (i.e., green and red).

3.2.1 Scandinavia

From 1992 to 2015 the development of agriculture and forest area in Scandinavia is in Figure 9 recognized with a net gain and loss, respectively. The latter, net forest loss, is minor compared to the net gain in agricultural land, but the aggregated gross loss and gain of forest changes are of greater magnitude than for agriculture. However, the maps displaying transitions between these two categories (Figure 11 and Figure 12) indicate that the total area gap between these two gross transitions in Norway explicitly, may not be that significant. Especially forest loss to agriculture is overrepresented in land outside of Norway (Figure 12). This transition is concentrated near populated areas in the southern parts of the area cut, such as south-eastern Norway. Whereas in northern and coastal land areas, the opposite development is more evident for Norway.

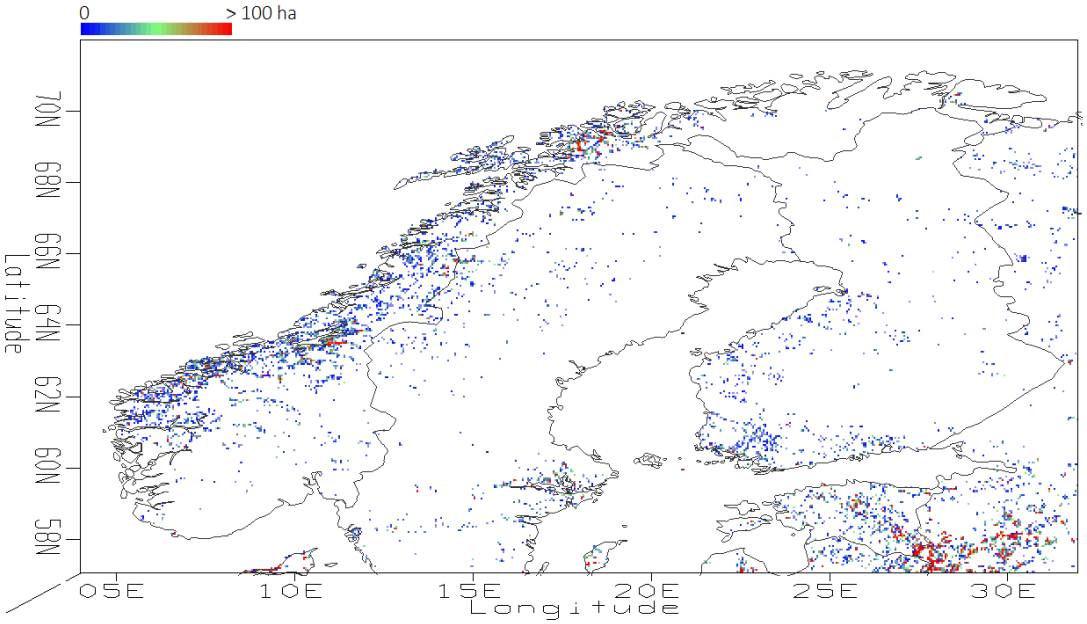

Figure 11. Spatial distribution of land cover transitioned from agriculture to forest in Scandinavia (1992-2015)

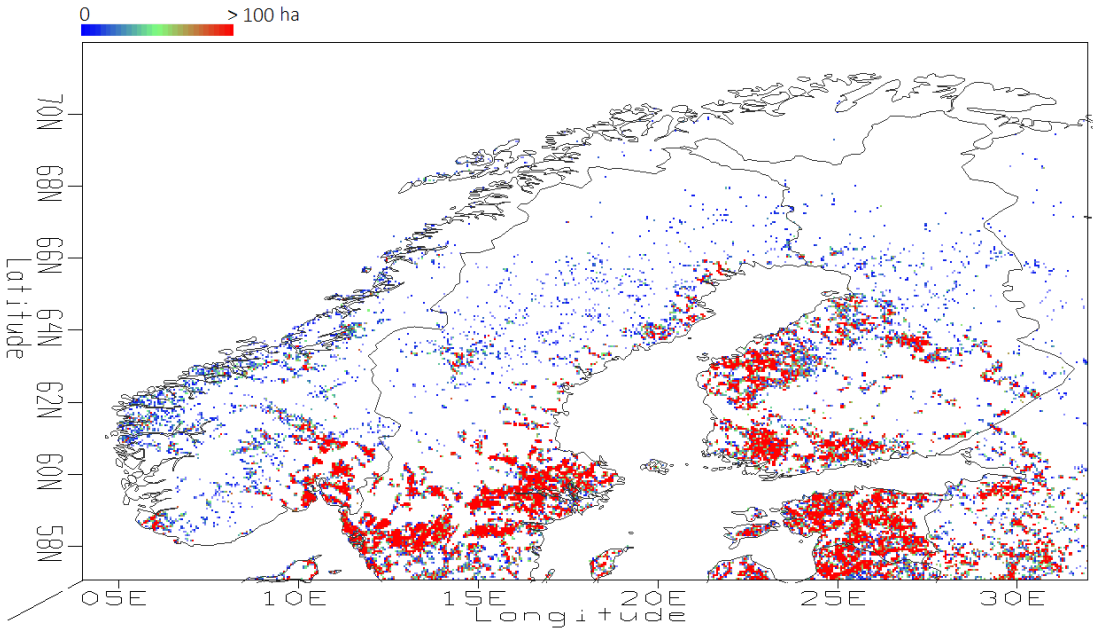

Figure 12. Spatial distribution of land cover transitioned from forest to agriculture in Scandinavia (1992-2015)

In addition to agriculture, forest transitions with grassland, water and wetland are also mapped. The latter is displayed in Figure 13 (Forest to Wetland) and Figure 14 (Wetland to Forest), which reveals a clear difference in the spatial distribution between these two LC changes. From Figure 9 it is already apparent that the forest gain from wetland is greater than the forest loss to wetland. Figure 14 identifies two major hot spot zones for the transition of wetland to forest, one in central Norway concentrated around the counties (fylke, in norwegian) Trøndelag and Møre og Romsdal and another more extensive one in the northern parts of Finland and Russia.

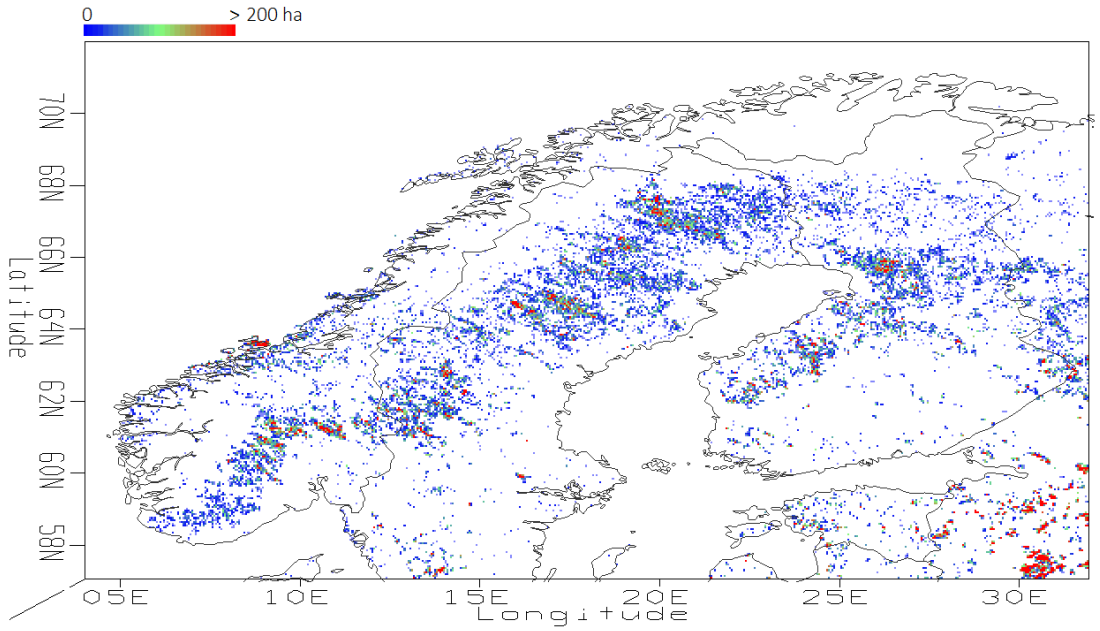

Figure 13. Spatial distribution of land cover transitioned from forest to wetland in Scandinavia (1992-2015)

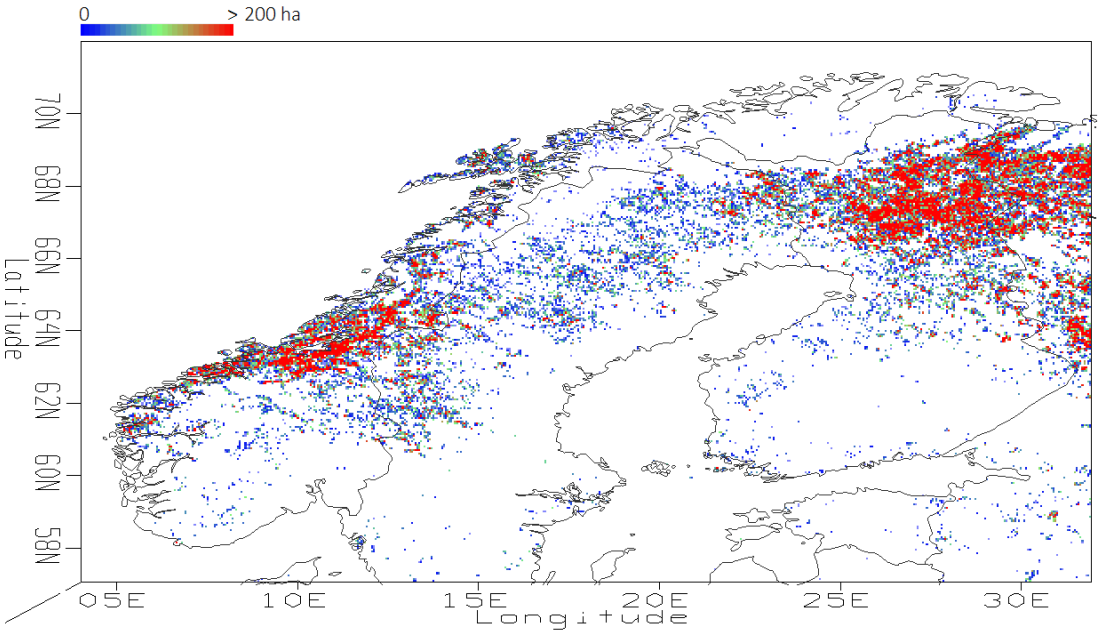

Figure 14. Spatial distribution of land cover transitioned from wetland to forest in Scandinavia (1992-2015)

Figure 15 and Figure 16 visualize the spatial pattern of grassland and forest interchanges. The maps demonstrate that most of the Norwegian forest area that transitioned to grassland during the study period was located mainly along the South-Eastern parts of the Scandes mountain range. Other than within Norway, this transition also unfolded in Estonia and Latvia. In the other direction however, grassland transitions to forest occurred almost exclusively along the Scandinavian mountains at higher latitudes.

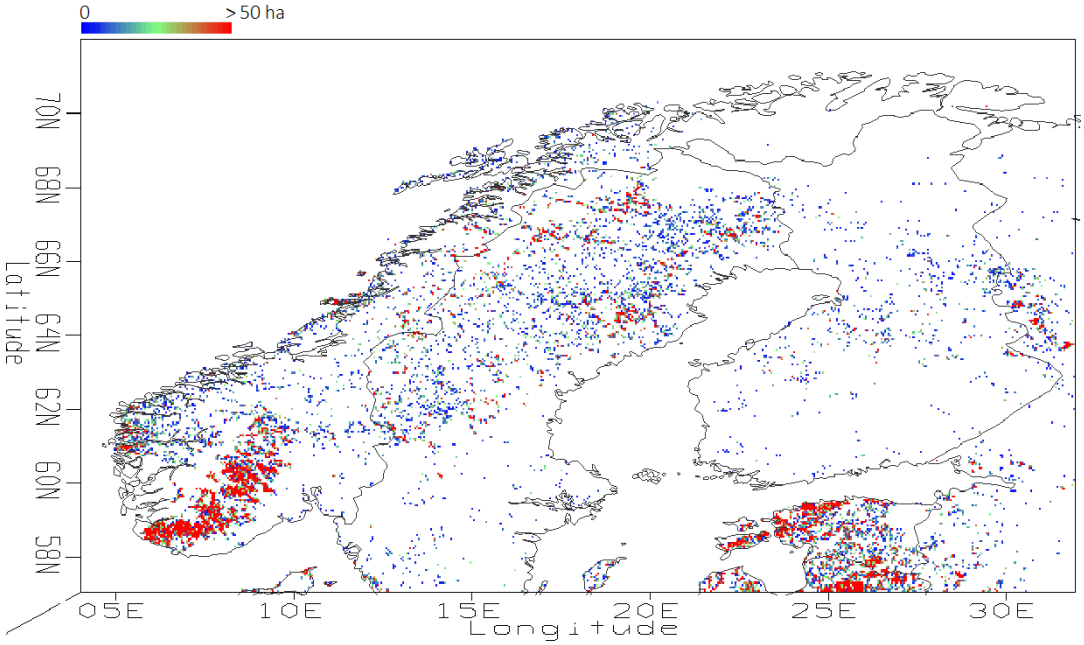

Figure 15. Spatial distribution of land cover transitioned from forest to grassland in Scandinavia (1992-2015)

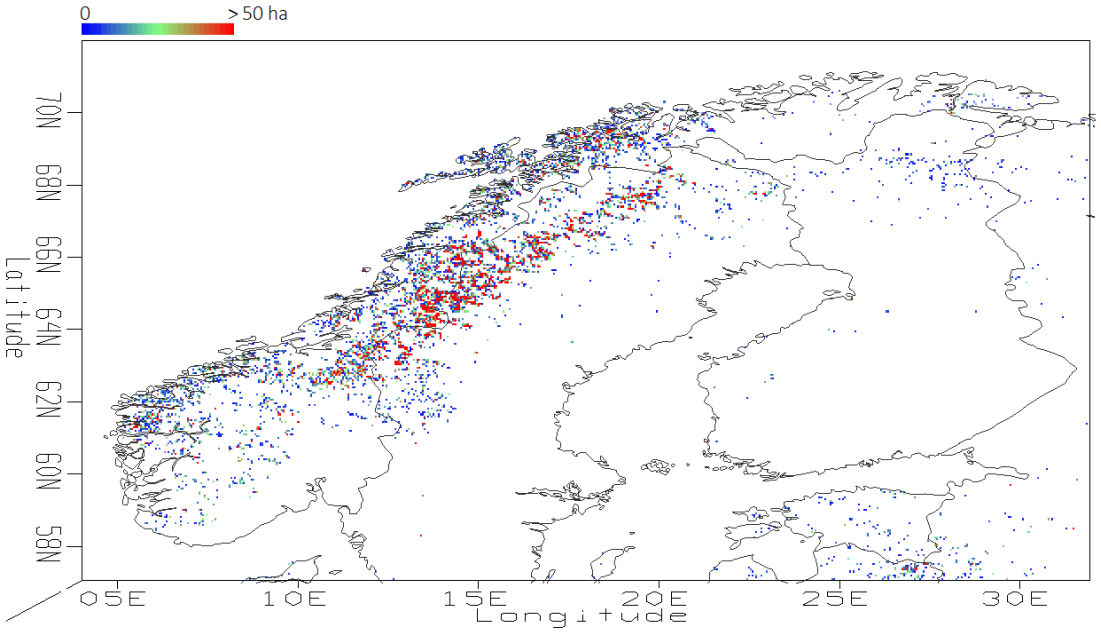

Figure 16. Spatial distribution of land cover transitioned from grassland to forest in Scandinavia (1992-2015)

Whereas forest to grassland transitions were most evident in the southern parts of Norway, the opposite is observed for the grassland gains from sparse vegetation. Illustrated by Figure 17 these LC changes can be

almost exclusively allocated to the most northern areas of Norway, Sweden and Finland.

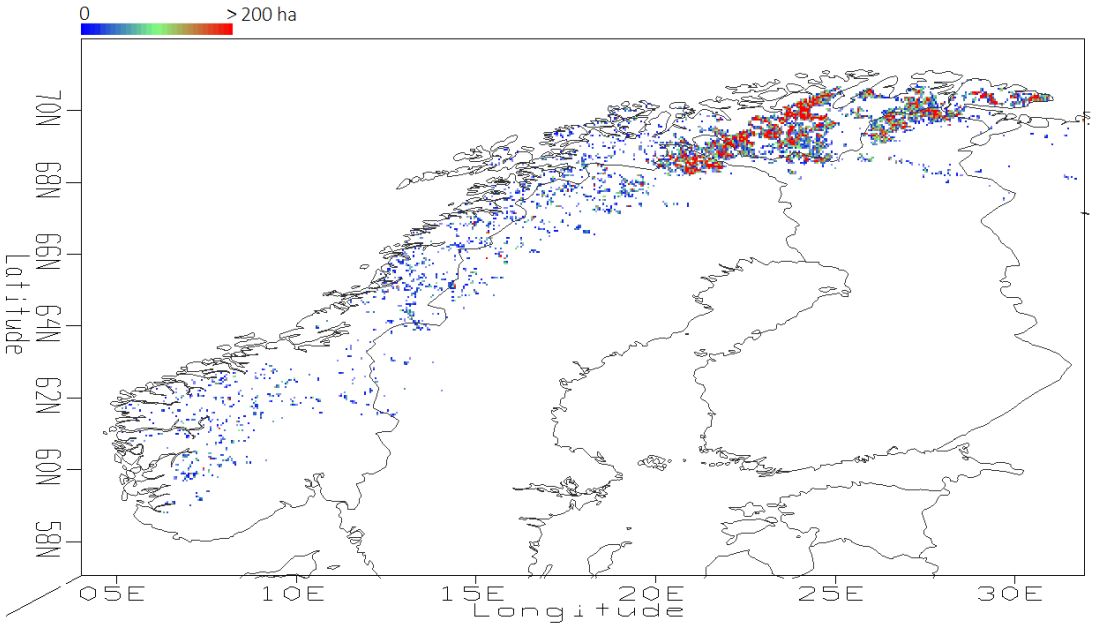

Figure 17. Spatial distribution of land cover transitioned from sparse vegetation to grassland in Scandinavia (1992-2015)

LC changes from forest to water and conversely, are displayed in Figure 18 and Figure 19. These show similar spatial distribution, but the water gain from forest is mainly distributed over inland areas whereas the forest gain from water seems to be more pronounced along the coastlines.

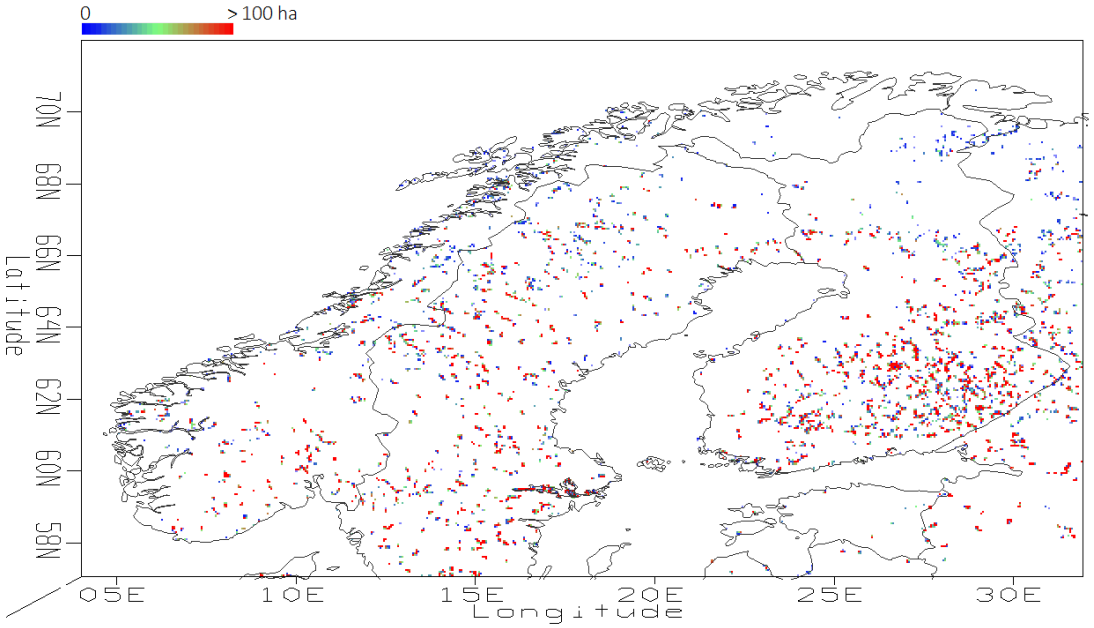

Figure 18. Spatial distribution of land cover transitioned from forest to water in Scandinavia (1992-2015)

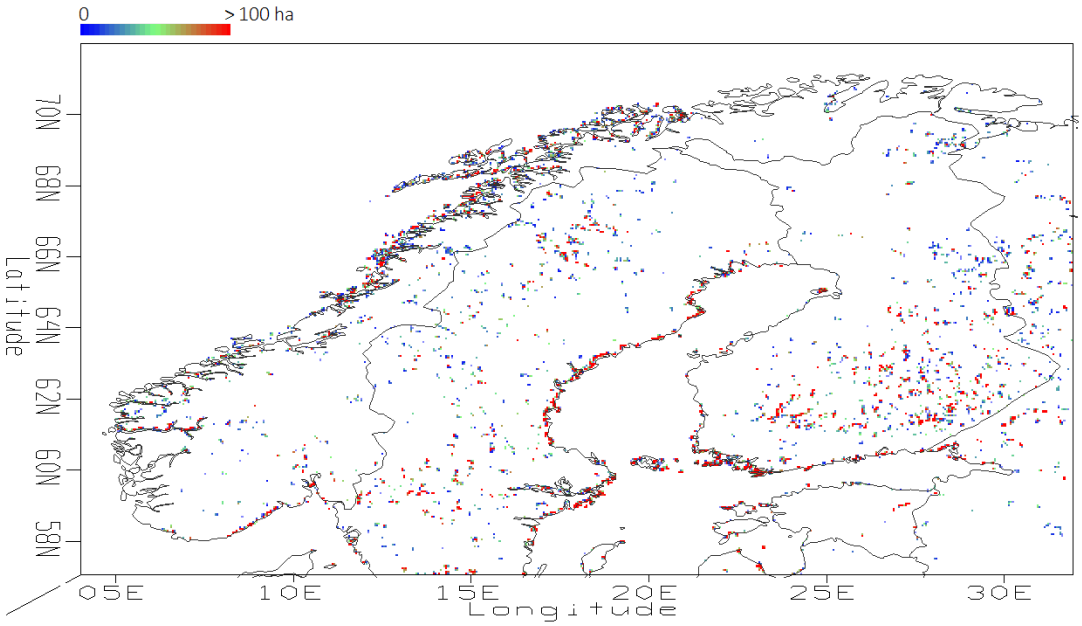

Figure 19. Spatial distribution of land cover transitioned from water to forest in Scandinavia (1992-2015)

3.2.2 Tibet

The maps generated for Tibet show that gross changes in agricultural land are of great spatial variety among the LC classes being the source of the change i.e., the agriculture transitions with forest (Figure 20 and Figure 21) have occurred in a distinctively different area than the grassland interchanges with agriculture (Figure 22 and Figure 23). Agricultural transitions with forest within the area cut are mainly located in Nepal and India. The gain of agricultural land from forest is characterized by an intensive hot spot close to and around Nepal's capital, Kathmandu.

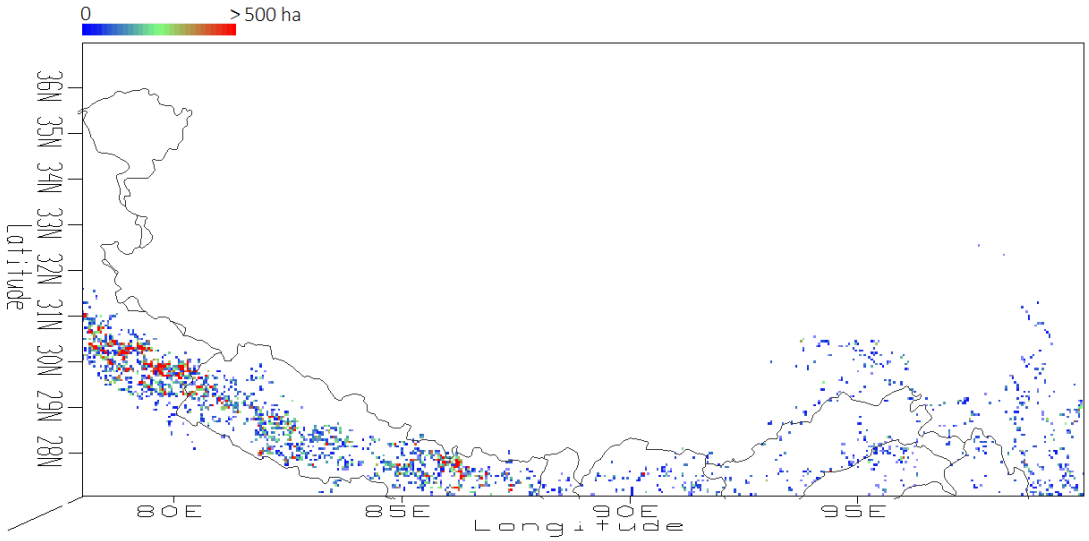

Figure 20. Spatial distribution of land cover transitioned from agriculture to forest in Tibet (1992-2015)

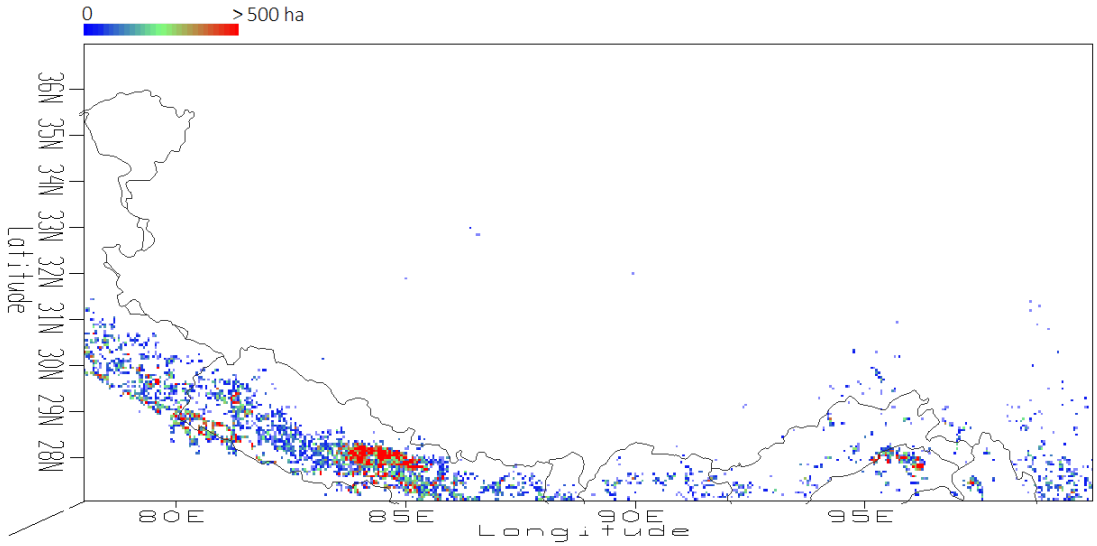

Figure 21. Spatial distribution of land cover transitioned from forest to agriculture in Tibet (1992-2015)

Agricultural interchanges with grassland however are more represented over the Tibetan Plateau and Chinese regions of the area cut. Once again, the agricultural gain is of a more intensive spatial character than the loss in agricultural land i.e., the LC change from grassland to agriculture seem to be centered in clusters to the east of the Plateau whereas grassland gain from agriculture is distributed across the area cut in a more spatially extensive pattern.

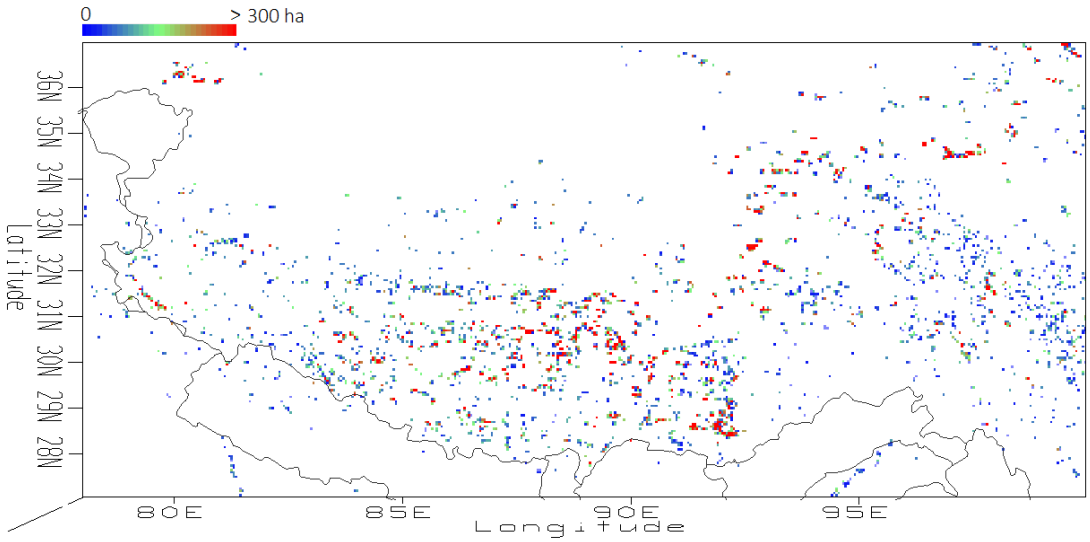

Figure 22. Spatial distribution of land cover transitioned from agriculture to grassland in Tibet (1992-2015)

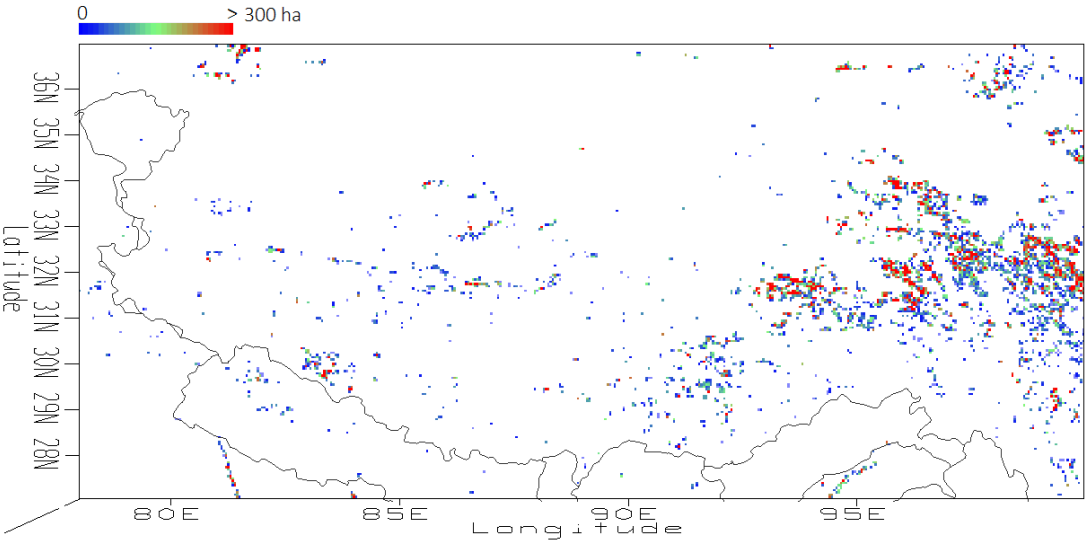

Figure 23. Spatial distribution of land cover transitioned from grassland to agriculture in Tibet (1992-2015)

The biggest gross and net area changes are found between grassland and bare area (Figure 10), and the related spatial distribution (Figure 24 and Figure 25) shows that these transitions mainly can be placed within the Tibetan Plateau. South and central parts of the Plateau and the northern corners, particularly to the north-east, mark zones of intensive change from bare area to grassland. A similar spatial pattern is seen for transitions from bare area to sparse vegetation (Figure 28) and sparse vegetation converted to grassland (Figure 27). Contrasting changes, of grassland converting to sparse vegetation (Figure 26) and bare area (Figure 25) are more concentrated in the central parts of the Plateau, especially to the north and west.

Lastly, a map was also created for water area gain from grassland, because this transition was responsible for 80 % of the significant net gain for water in the study period (net gains/losses can be studied in Table 9). This LC change took place in the central areas of the Plateau.

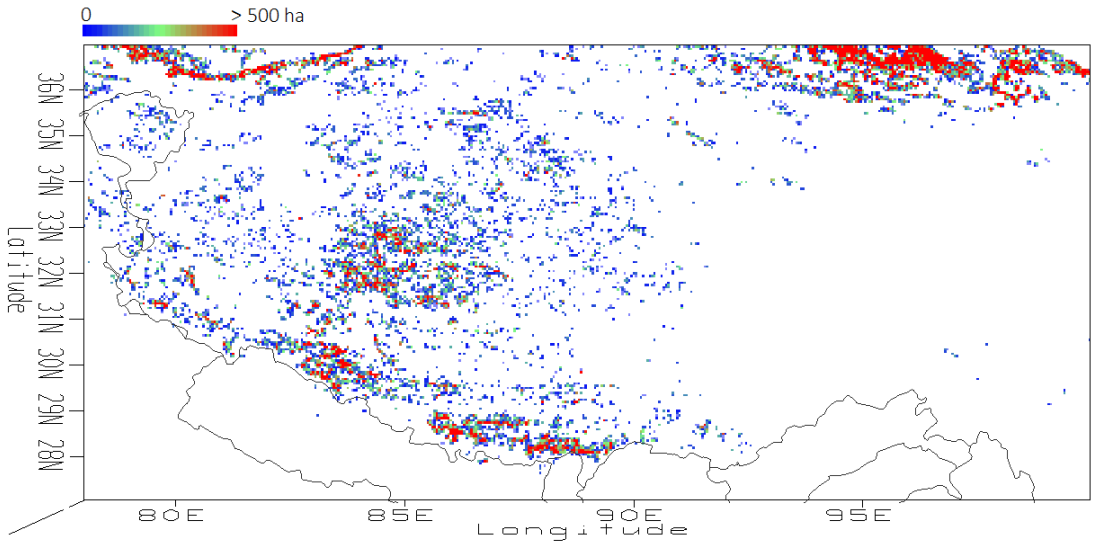

Figure 24. Spatial distribution of land cover transitioned from bare area to grassland in Tibet (1992-2015)

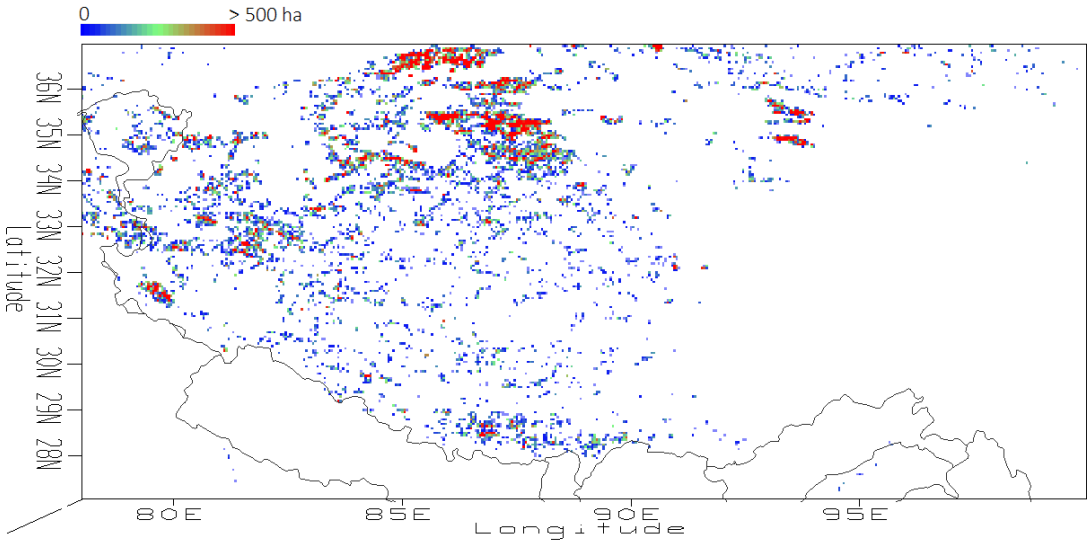

Figure 25. Spatial distribution of land cover transitioned from grassland to bare area in Tibet (1992-2015)

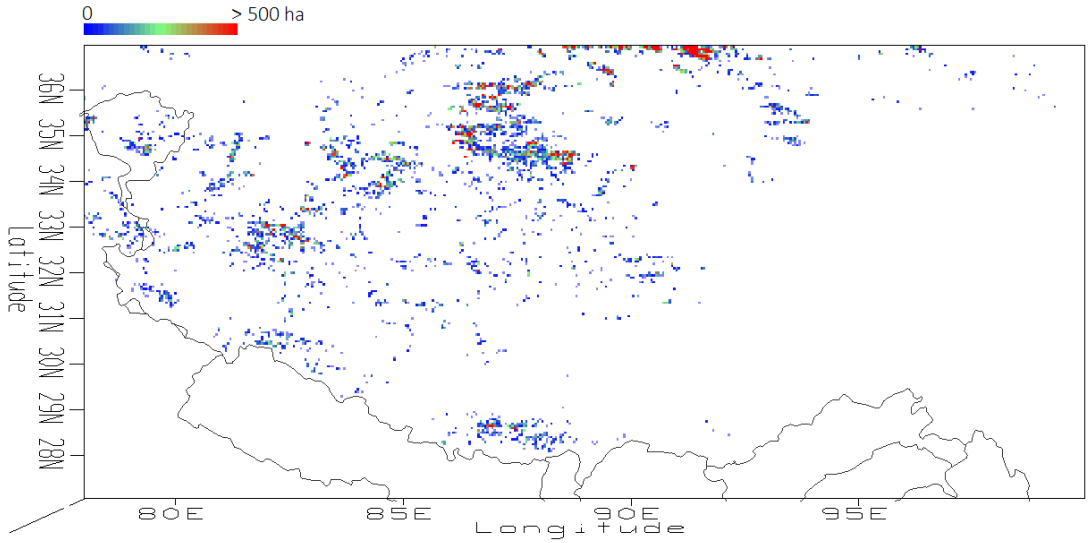

Figure 26. Spatial distribution of land cover transitioned from grassland to sparse vegetation in Tibet (1992-2015)

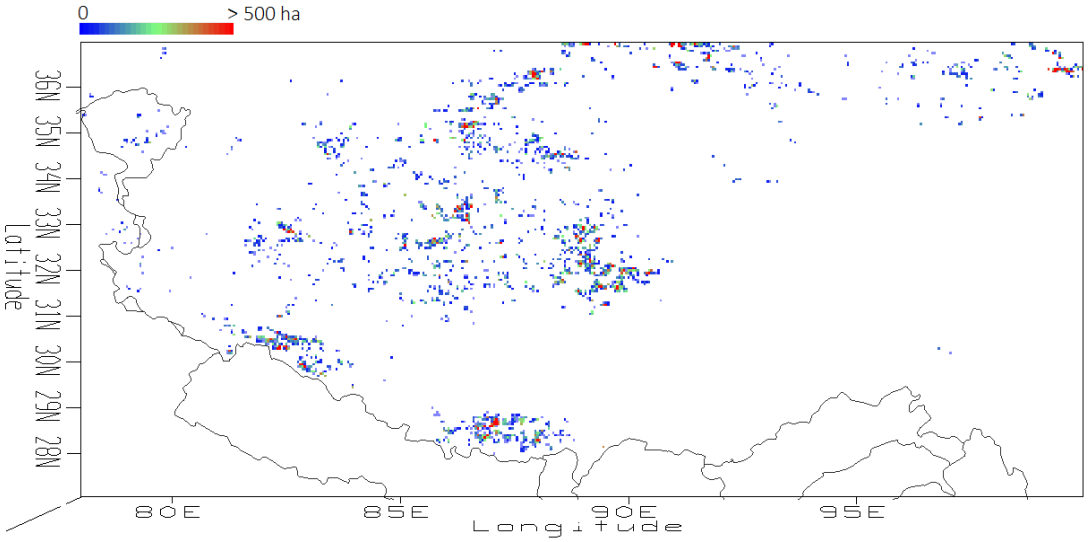

Figure 27. Spatial distribution of land cover transitioned from sparse vegetation to grassland in Tibet (1992-2015)

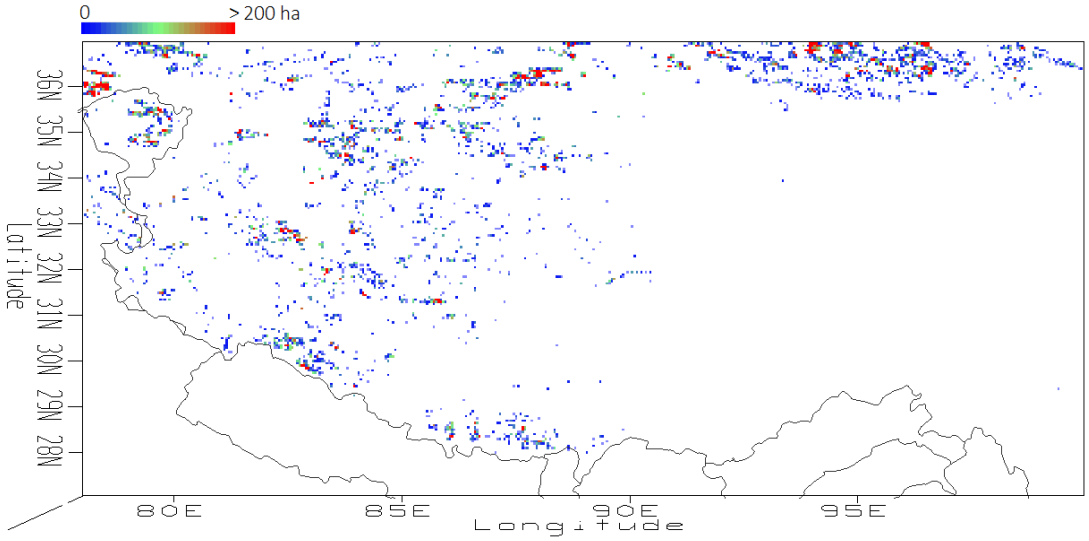

Figure 28. Spatial distribution of land cover transitioned from bare area to sparse vegetation in Tibet (1992-2015)

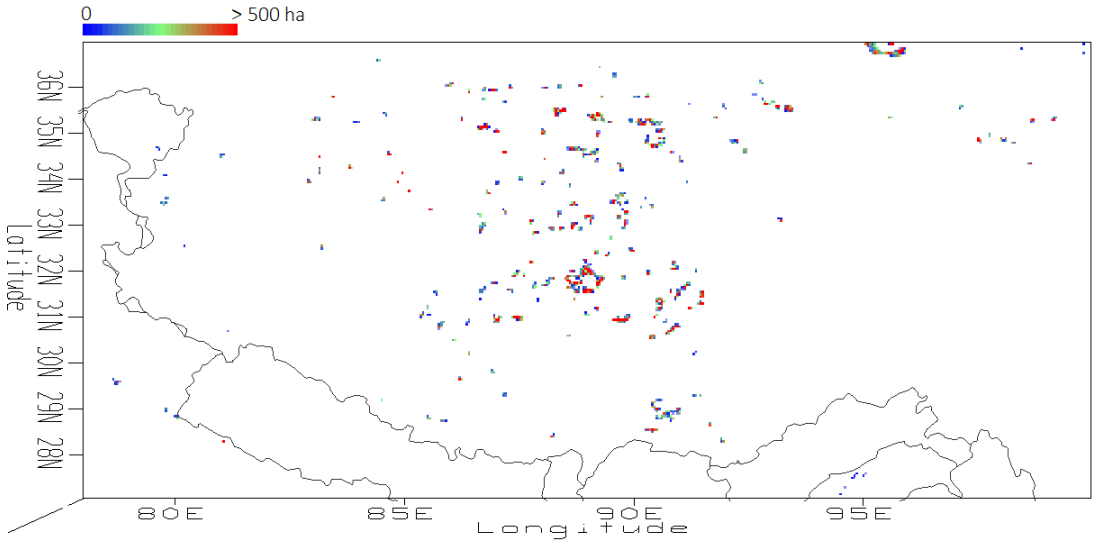

Figure 29. Spatial distribution of land cover transitioned from grassland to water in Tibet (1992-2015)

3.3 Time series analysis

Area charts and trend lines were generated for comparison among different LC changes and to visualize how the total area of individual LC types changed on a year-to-year basis over the study period. An area chart for water is not created for Scandinavia, as it would not be sensible to draw conclusions on total area of inland water bodies from values that also account for (without separating) total area of ocean water in the area cut. Area charts for LC classes that are focused on in the discussion in section 4 are included in this section; the rest can be found in appendix B. Attention should be paid to the scale on the vertical axis of the area charts for each LC category, which differs between the charts that are horizontally aligned. It extends from the minimum area value to the maximum area value in the close-up figure (on the right-hand side) and from zero in the figure on the left-hand side. Values of yearly area for all LC classes are listed in Table 8 in the appendix.

Trend lines for the gross LC changes of greatest absolute magnitude were computed. Figure 41 and Figure 42 show trend for the major transitions in Scandinavia and Tibet, respectively. The trend lines were plotted for both "directions" of the transition even if one of these did not make a major contribution e.g., agriculture to forest was included although it is of a much lower magnitude than the reciprocal change, forest to agriculture. Each yearly dot marker (circle) of a specific LC change is the value of how much area changed from one LC class to another during the year that the dot marks (e.g., if the dot marks year 2000, this value is the area change that occurred in 2000, comparing yearly area data in 2000 with the corresponding area in 2001).

The area charts demonstrate the results obtained in Table 5 (area changes relative to each LC type) distributed yearly over the study period. It is also easy to detect which LC classes that have had a development characterized by big absolute and relative changes.

Forest development in both regions exemplify a relatively steady state (Figure 30, Figure 31), with both increases and decreases.

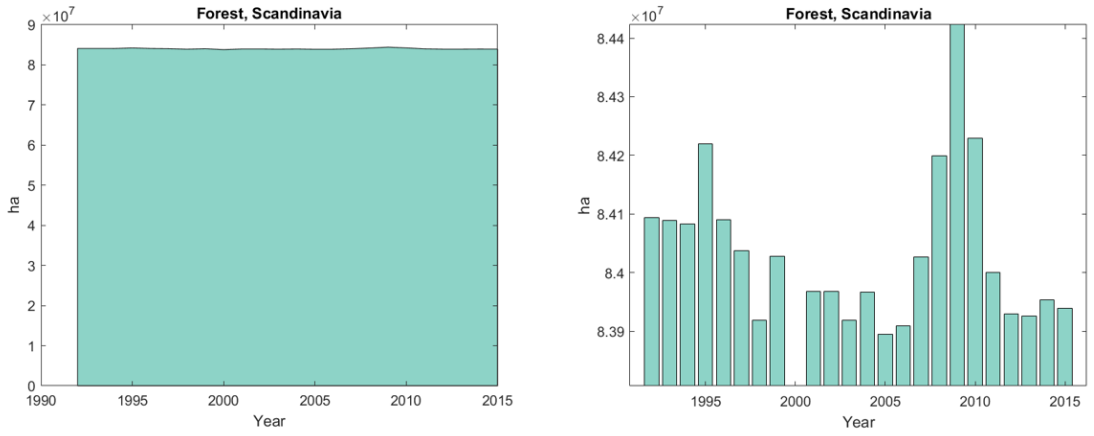

Figure 30. Total forest area (in hectares) in Scandinavia 1992-2015. Both charts display the exact same data, but the chart on the right-hand side differs from from the one to the left by its vertical axis, that spans from the minimum to the maximum value, whereas the left chart's axis starts at zero. As such, the charts indicate the year-to-year change pattern (trend) and magnitude of the change relative to total area.

Agriculture and grassland area in Scandinavia show a stable growth trend strikingly similar to each other (Figure 32, Figure 33), with especially accelerated growth around year 2000, 2004 and 2010.

The agricultural development in Tibet is not that big relative to the agriculture area in 1992, but Figure 34 shows that a significant increase could be observed in 1999 and 2000, and after this a steady decline followed.

Similarly, total grassland area has been stable in Tibet. However, a characteristic development of first a decreasing trend followed by a greater increase has been seen in the study period.

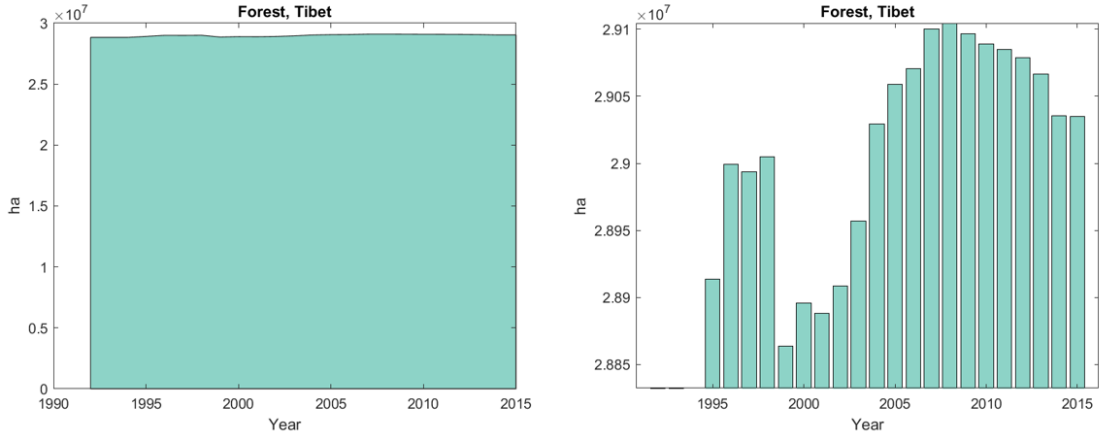

Figure 31. Total forest area (in hectares) in Tibet 1992-2015. Both charts display the exact same data, but the chart on the right-hand side differs from from the one to the left by its vertical axis, that spans from the minimum to the maximum value, whereas the left chart's axis starts at zero. As such, the charts indicate the year-to-year change pattern (trend) and magnitude of the change relative to total area.

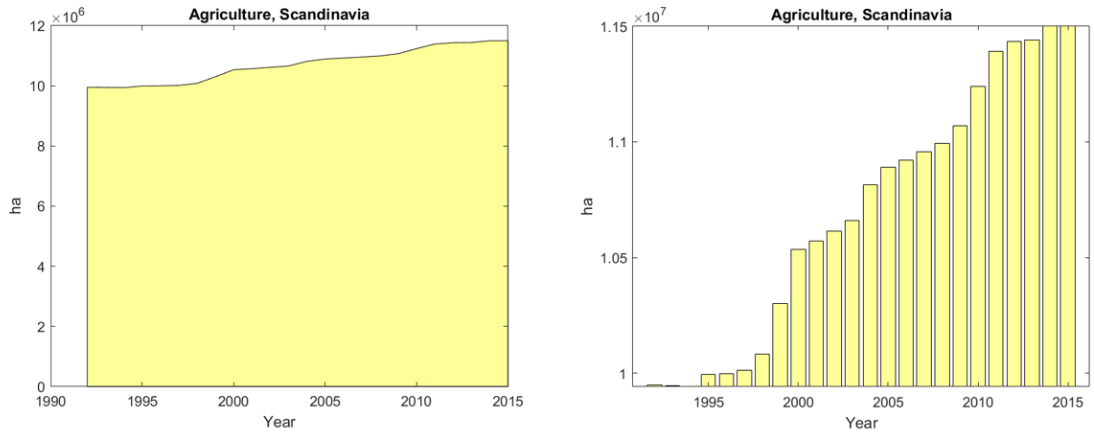

Figure 32. Total agricultural area (in hectares) in Scandinavia 1992-2015. Both charts display the exact same data, but the chart on the right-hand side differs from from the one to the left by its vertical axis, that spans from the minimum to the maximum value, whereas the left chart's axis starts at zero. As such, the charts indicate the year-to-year change pattern (trend) and magnitude of the change relative to total area.

The most characteristic growth pattern is noted for the settlement class, which for both study regions show a stable increase. Whereas a flattening tendency is seen in Scandinavia settlement towards the end of the study period (Figure 36), the development in Tibet is of a more exponential character (Figure 37).

The LC classes that stands out in terms of net area losses are wetland in Scandinavia (Figure 38) and bare area in Tibet (Figure 39), as also noted in the previous analysis in subsection 3.1. These show a consistent decline, reaching the lowest area of the study period in the last years, 2014-2015. The opposite is the case for water changes in Tibet (Figure 40); a steadily increase in water area lead to the highest values being observed in 2014-2015.

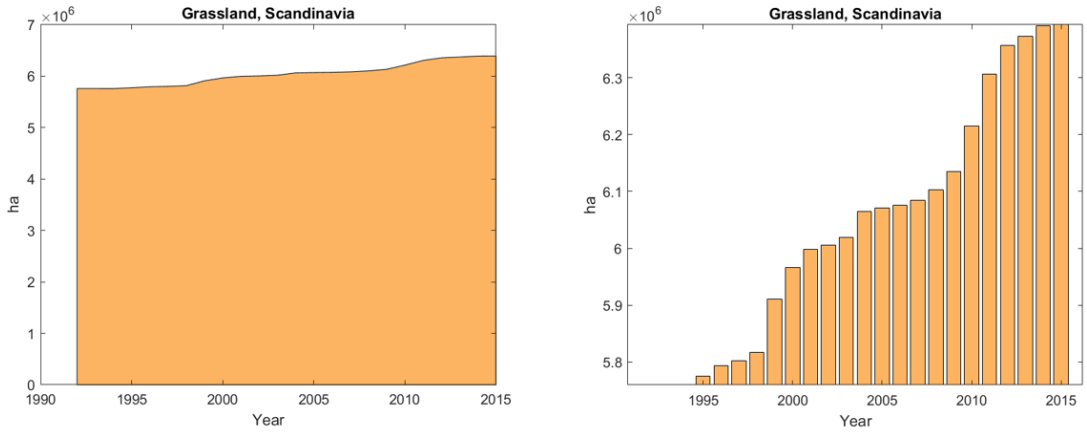

Figure 33. Total grassland area (in hectares) in Scandinavia 1992-2015. Both charts display the exact same data, but the chart on the right-hand side differs from from the one to the left by its vertical axis, that spans from the minimum to the maximum value, whereas the left chart's axis starts at zero. As such, the charts indicate the year-to-year change pattern (trend) and magnitude of the change relative to total area.

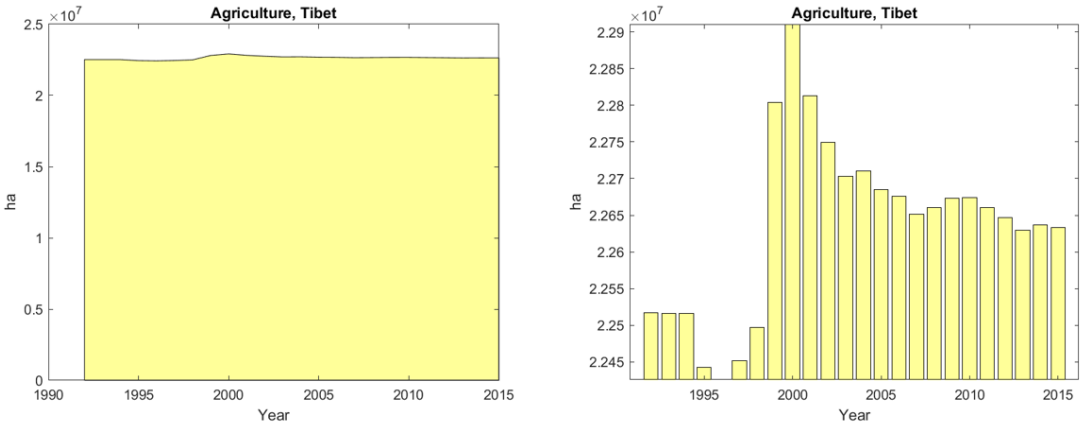

Figure 34. Total agricultural area (in hectares) in Tibet 1992-2015. Both charts display the exact same data, but the chart on the right-hand side differs from from the one to the left by its vertical axis, that spans from the minimum to the maximum value, whereas the left chart's axis starts at zero. As such, the charts indicate the year-to-year change pattern (trend) and magnitude of the change relative to total area.

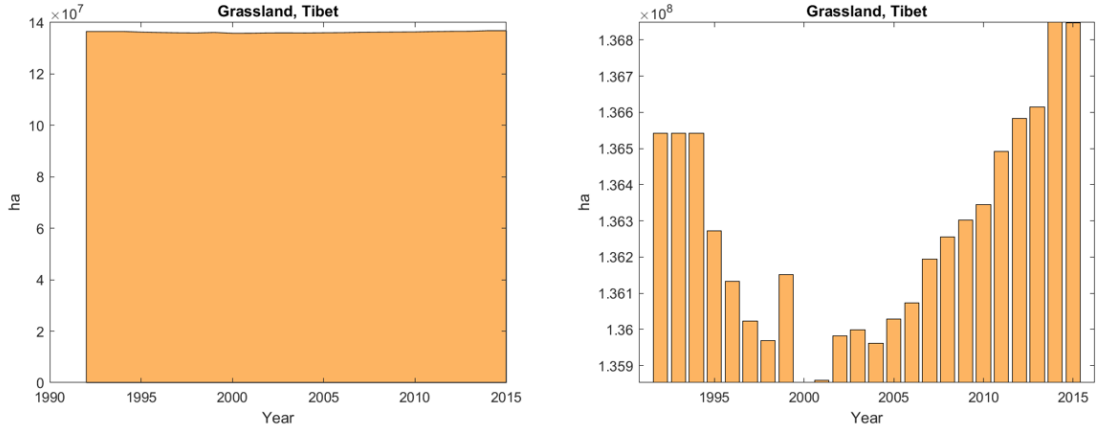

Figure 35. Total grassland area (in hectares) in Tibet 1992-2015. Both charts display the exact same data, but the chart on the right-hand side differs from from the one to the left by its vertical axis, that spans from the minimum to the maximum value, whereas the left chart's axis starts at zero. As such, the charts indicate the year-to-year change pattern (trend) and magnitude of the change relative to total area.

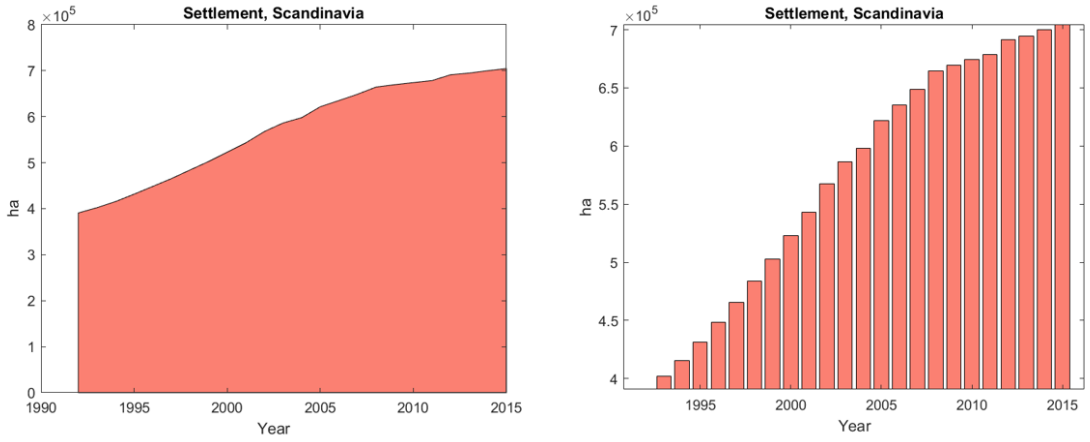

Figure 36. Total settlement area (in hectares) in Scandinavia 1992-2015. Both charts display the exact same data, but the chart on the right-hand side differs from from the one to the left by its vertical axis, that spans from the minimum to the maximum value, whereas the left chart's axis starts at zero. As such, the charts indicate the year-to-year change pattern (trend) and magnitude of the change relative to total area.

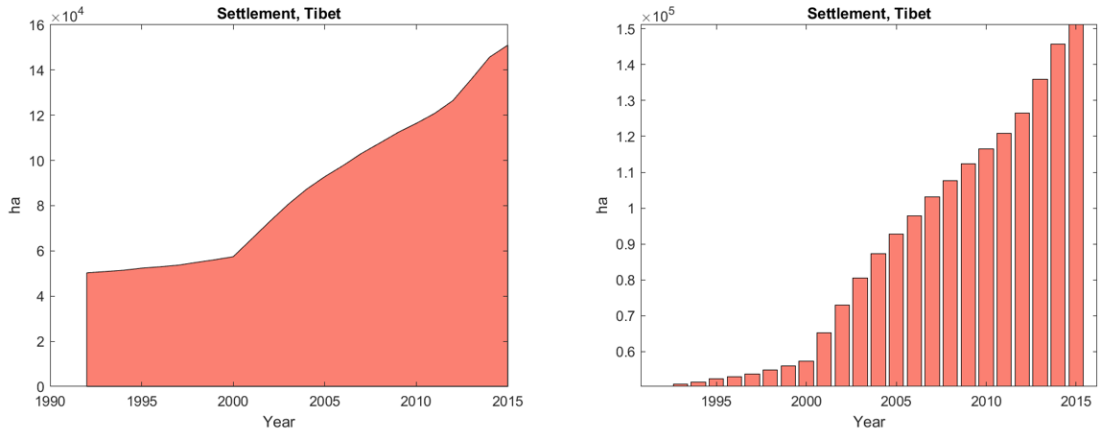

Figure 37. Total settlement area (in hectares) in Tibet 1992-2015. Both charts display the exact same data, but the chart on the right-hand side differs from from the one to the left by its vertical axis, that spans from the minimum to the maximum value, whereas the left chart's axis starts at zero. As such, the charts indicate the year-to-year change pattern (trend) and magnitude of the change relative to total area.

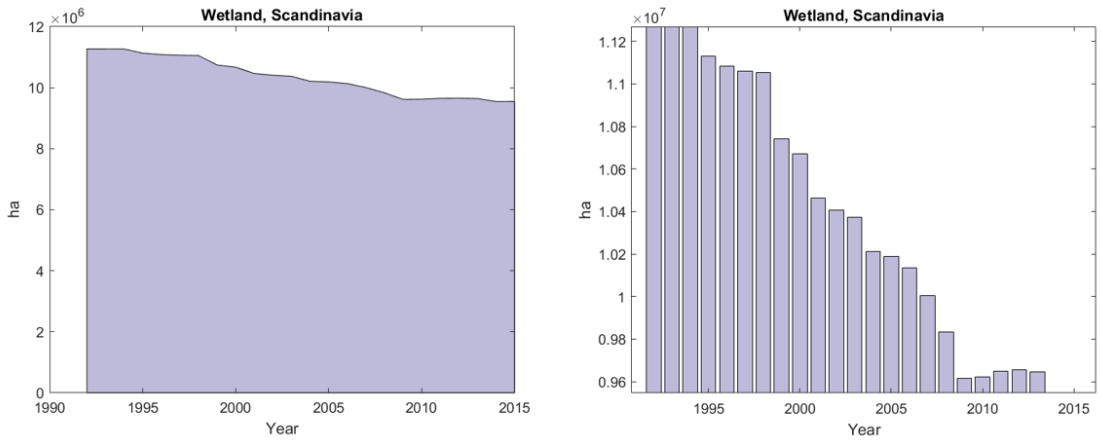

Figure 38. Total wetland area (in hectares) in Scandinavia 1992-2015. Both charts display the exact same data, but the chart on the right-hand side differs from from the one to the left by its vertical axis, that spans from the minimum to the maximum value, whereas the left chart's axis starts at zero. As such, the charts indicate the year-to-year change pattern (trend) and magnitude of the change relative to total area.

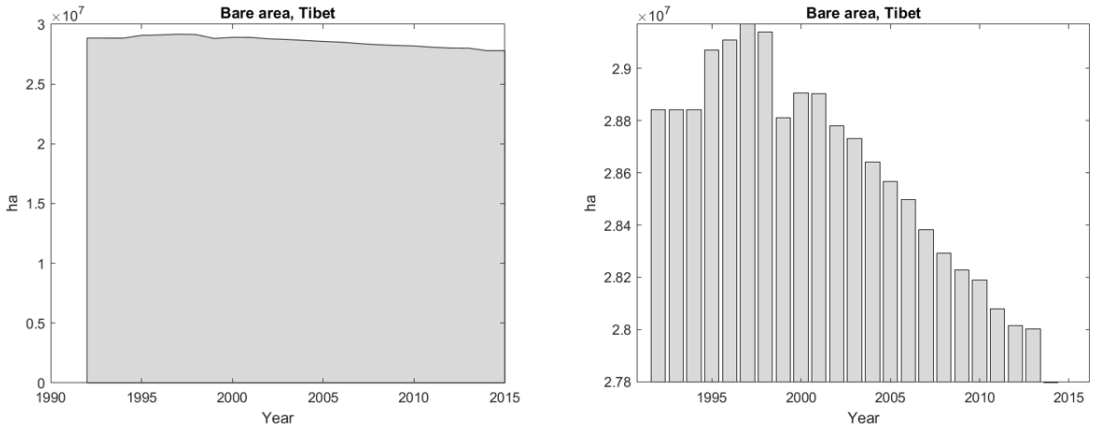

Figure 39. Total of bare area (in hectares) in Tibet 1992-2015. Both charts display the exact same data, but the chart on the right-hand side differs from from the one to the left by its vertical axis, that spans from the minimum to the maximum value, whereas the left chart's axis starts at zero. As such, the charts indicate the year-to-year change pattern (trend) and magnitude of the change relative to total area.

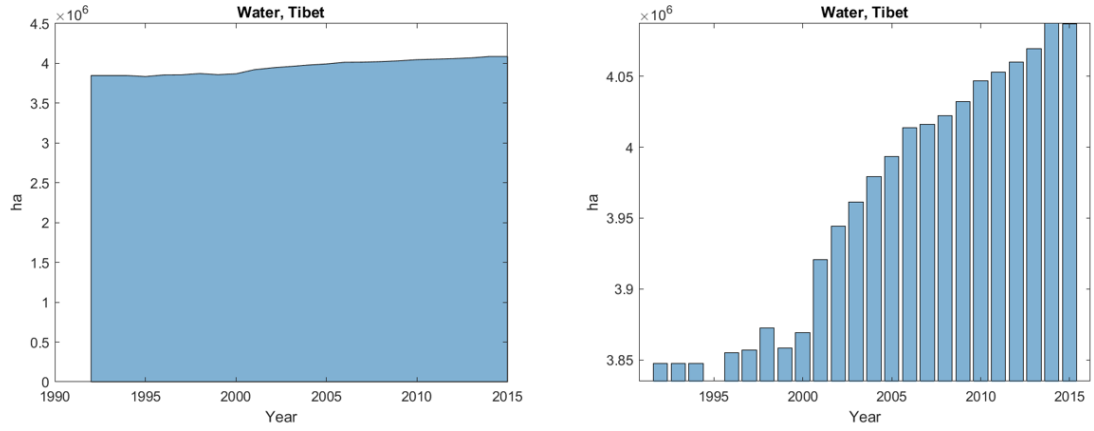

Figure 40. Total area of water (in hectares) in Tibet 1992-2015. Both charts display the exact same data, but the chart on the right-hand side differs from from the one to the left by its vertical axis, that spans from the minimum to the maximum value, whereas the left chart's axis starts at zero. As such, the charts indicate the year-to-year change pattern (trend) and magnitude of the change relative to total area.

A direct comparison between Scandinavia and Tibet is not the intention of the trend charts, and it should be noted that the charts (and trend line colors) for the two regions do not consider the same transitions. However, some similarities may be of interest for discussion, such as the peak observed in year 1998 for transitions "wetland to forest" and "bare area to grassland" for Scandinavia (Figure 41) and Tibet (Figure 42), respectively. Other than this particular high value, there are characteristic but smaller peak values associated with several of the transition types for both regions especially in the years 1994, 1998-2000, 2003 and 2013. In Scandinavia, changes from wetland to forest are also prominent from 2006 to 2009. Forest gain from agriculture seems to have followed a similar change pattern, with the most recent changes lagging a bit in time behind the wetland to forest changes. In Tibet, transitions between agriculture and grassland seem to have occurred mainly within a short period of time and almost concurrently (mostly in 1997-2004).

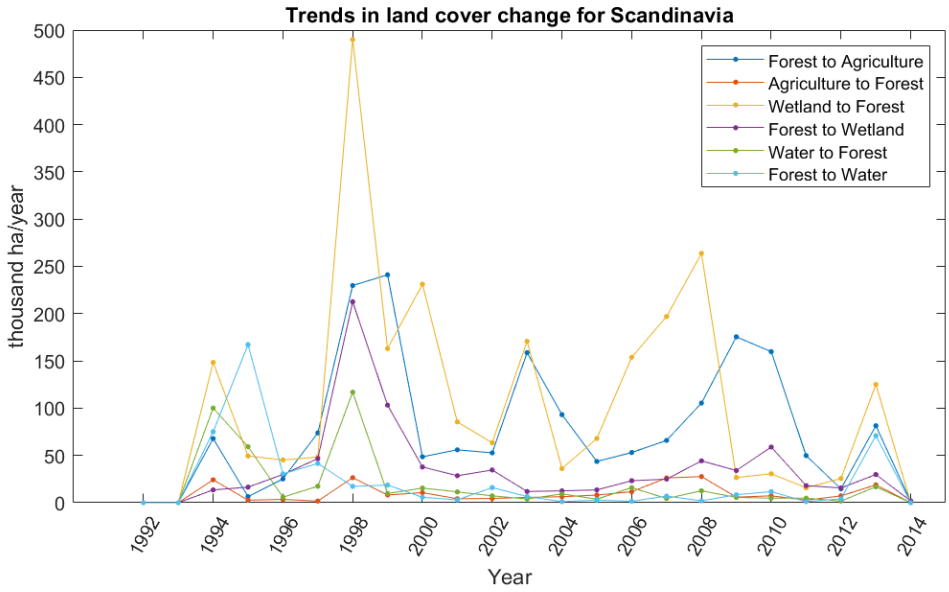

Figure 41. Land cover transition trends from 1992 to 2015 for Scandinavia. Each circular marker represents the gross LC change that occurred within that year e.g. the marker for year 2000 represents LC change that occurred from the beginning of year 2000 to the beginning of year 2001.

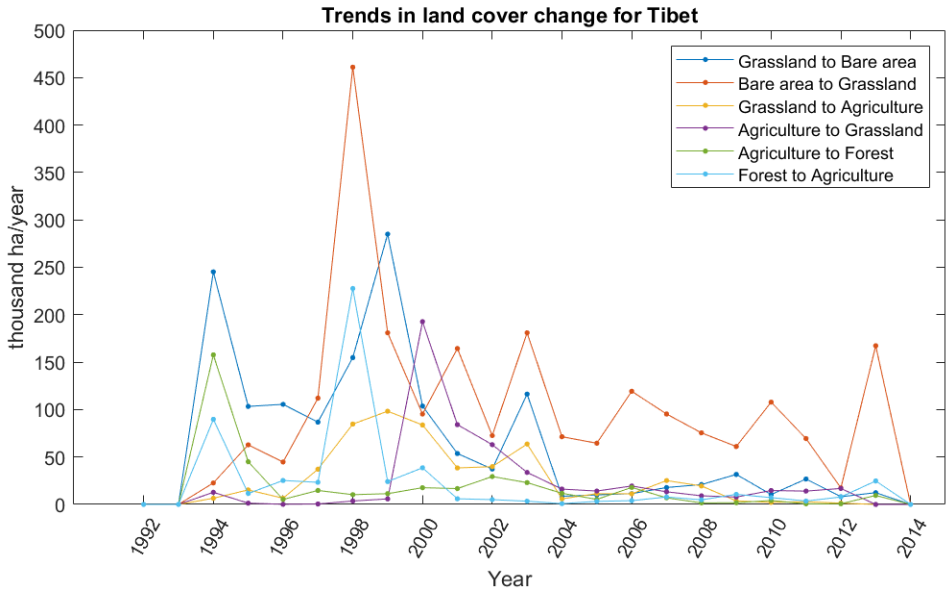

Figure 42. Land cover transition trends from 1992 to 2015 for Tibet. Each circular marker represents the gross LC change that occurred within that year e.g. the marker for year 2000 represents LC change that occurred from the beginning of year 2000 to the beginning of year 2001.

4 Discussion

4.1 Results

The objective of study was achieved through three complementing analytical approaches and the results from these, namely the absolute gross and net transition analysis in subsection 3.1, spatial analysis in subsection 3.2 and temporal analysis in subsection 3.3. In correspondence with the research questions stated in subsubsection 1.2.1, the major LC changes in the two regions of study will in this section be discussed in light of recent land use and possible drivers.

4.1.1 Scandinavia

Agricultural development

The biggest net change in Scandinavia over the study period (1992-2015) was the gain in agricultural land. 1.6 million hectares indicates a significant expansion of the agriculture sector. The development seems sensible considering a continuous growing population in the Scandinavian countries [38], which is probably also the main driver of the increase in settlement area. As the population grows, more infrastructure and housing is needed, augmenting the area requirements for the settlement. Similarly, a higher demand for food naturally arises from the population increase, and this requires land for agricultural production. The biggest sacrifice in this regard was found in the forest class (Figure 9); forest area lost to agricultural land also represents the greatest forest loss in the region. The net decline of 155 thousand hectares is however small compared to total forest area (only 0.19 % of the forest cover in 1992). Furthermore, the spatial analysis in subsection 3.2 revealed that this transition mostly took place outside of Norway, so a net growth of agricultural land in Norway cannot actually be concluded from these results alone. This emphasizes the importance of the spatial analysis and the application of a datamask for country-specific studies.

Despite a clear trend in climate-influenced forest growth, altered land use in the form of abandoned land patches previously occupied for human use is argued to be the major cause of the forest expansion seen in Norway during recent decades [39, 24]. The data used in this thesis is from recent time, so the results clearly do not capture direct forest regrowth from older agricultural land use. However, Figure 11 demonstrates that forest growth has occurred on recently cultivated land, especially pronounced around Trøndelag county. This area has an active and ambitious forestry sector with a steadily increasing annual forest volume [40], which may explain the transitions from agricultural land to forestry, considering at the same time the ongoing agricultural intensification trend [32, 30].

Declining wetlands

In contrast to the mapped agricultural-forest transitions, where no clear growth tendency could be demonstrated for Norway explicitly, wetland interchanges with forest are more distinguishable. These point to a clear net increase of forested land, both for Norway and the total area cut, just as expected from the initial net transition analysis (Figure 9) in subsection 3.1. A large share of wetland transitions to forest took place in Norway (Figure 14), and with a net area of 1.6 million hectares changing from wetland to forest between 1992 and 2015 this is the most important contribution to (gross) forest growth in Scandinavia. Within Norway, the hot spot of wetland change (to forest) is found in the central region. This is not surprising, as this is where most of the existing and new growth has occurred according to area surveys [11]. It is difficult to check consistency of the wetland area data from the CCI-LC satellite data with literature findings from land or aerial based field surveys because these are conducted over several years, and as such does not measure yearly changes, and also usually performed on a country basis and can as such not be directly compared with the area cut of this study. Wetland is furthermore a LC class that previously has been underestimated in Norwegian national statistics, by as much as one million hectares according to a land cover (area frame) survey performed between 2005 and 2014 [11]. What is apparent however, is the clear tendency of declining wetlands and the fact that this is an important source of GHG emissions and hence climate change [2]. This emphasizes the need for knowledge on the drivers behind these changes, in order to create and implement of effective policies and measures. The Swedish Wetland Survey from 2009 [27] lists various factors that been

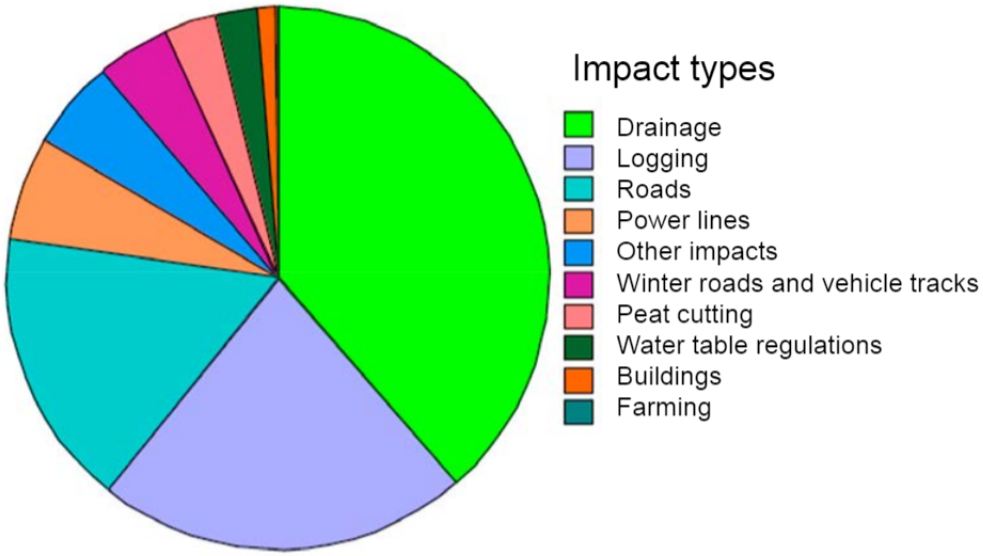

Figure 43. Registered proportions of different anthropogenic impact types on Swedish wetlands [27]

damaging on wetland ecosystems (Figure 43). Due to similarities in geography and topography of Norway and Sweden it is reasonable to believe that these findings are highly transferable to the Norwegian context, especially considering that the three major impact categories (drainage, logging and roads) are related with forestry activities prevalent in Norway has [25]. Climate change may also be a contributing factor of wetland degradation, due to higher average temperatures observed the last decades [41]. Climate change effects are predicted to be more prevalent in the future, especially considering that some wetland types are highly sensitive to climate conditions [27].

The wetland trend however seems to be more optimistic towards the end of the study period, as the wetland area stabilizes from year 2009 (Figure 38). This may imply that conservation efforts are leveling the observed degradation trends, and will possibly surpass these as conservation policies improve and disseminate in a greater scale.

Forest and grassland changes

Studies indicate that climate and anthropogenic drivers are pushing forest limits in Norway to higher altitudes [39]. This may explain some of the observed forest gain from grassland and sparse vegetation. The distribution of forest converted to grassland is more characteristic (Figure 15) however. It shows that there has been a large shift from forested land to grasslands in the subalpine areas in the south of Norway. This change could possibly be the result of forest thinning for forestry or changes in the local growing conditions or climate.

Among all the studied LC classes, grassland has the second biggest net gain in Scandinavia (second to agriculture). Net area gains from sparse vegetation to grassland and forest (Figure 9) suggests the occurrence of greening, which may be caused by recent temperature increase in Norway [41] that likely has improved the growing conditions and extended the growing season for vegetation in the north. This is seen from the northerly located hot spot in Figure 17.

4.1.2 Tibet

Urbanization

The Tibet area cut show signs of urbanization tendencies similar to that of Scandinavia. Despite that settlement represented only 0.07 % of total area in the Tibet area cut in 2015 (0.02 % in 1992), the relative increase

of nearly 200 % is substantial, especially considering other possible human land use changes correlated with the growth in settlement. A growth in settlement may also suggest that other types of LC and ecosystems will be impacted due to an increase in the demand for goods and services. Agricultural land represented 10 % of total area both in 1992 and 2015, so there has not been a big net change during the study period. However, there has been a shift in location of production. This can be seen by studying the maps of the major agricultural transitions i.e., the gains and loss with grassland and forest, spatially displayed in sub-subsection 3.2.2. Agricultural changes with forest are mostly located outside the Tibetan Plateau, in Nepal and India. Here, there is a tendency of agricultural production being more concentrated than in 1992, with a major hot spot near the highly populated Kathmandu. More forest were converted to agricultural land than what was gained from agriculture. The results do not imply a shift of previously cultivated land being abandoned, but rather an increase in the total production and a tendency that the most recent production is taking place around the most populated areas. The spatial intensification observed for agricultural land in Nepal is sensible considering that the country's capital area, Kathmandu Valley, has been experiencing one of the most rapid urbanization growths in South Asia [42].

For the Tibetan Plateau, it is more interesting to study the spatial distribution of the transitions between grassland and agriculture which are the most prominent LC changes related to agriculture within the Plateau. The results suggest a similar spatial development as in Nepal in terms of a more centralized agricultural production, demonstrated by changes from grassland area, which is the major source of the agricultural area gain at the Plateau. A comparison between the mapped gross transitions (gains and losses) between grassland and agriculture in Tibet (Figure 22 and Figure 23), indicates a shift in land use practices from extensive or rural agriculture to more intensive land cultivation concentrated in the eastern parts of the Plateau. The depopulation of grasslands on the Tibetan Plateau [22] is probably the major cause of this geographical shift. In efforts to protect biodiversity, ecology and ensure future water resources for the region, Chinese government lead policies have moved thousands of herders from their traditional lands into urbanized parts of the Plateau. The sudden accelerated growth in grassland from agriculture in year 2000 may be a sign that the effects of the early initiated grassland conservation projects have had rapid desired effects (Figure 42). On the other hand, the displacement of original settlements also has socioeconomic challenges for many. These issues are some places being actively addressed through so-called community co-management of natural resources, which may be the best-fit solution in a place in crucial of both conservation and socioeconomic development [22]. Besides land requirements for agriculture, settlement, transportation (roads and railways) and other infrastructure, there are further land use impacts associated with the increase in the tourism industry that has accelerated the demand within all these categories and hence exerts great stress on the terrestrial ecosystems on the Tibetan Plateau [10].

Grassland variations

Besides grassland interchanges with agricultural land, LC changes of an even bigger extent were detected between bare area and grassland. Grassland experienced the strongest gain, with a major hot spot located in the north-east of the plateau, where a highly intensive grassland growth has occurred. Other hot spot areas can be identified to the north-west and central area. The latter central area is located at a much higher elevation (altitude) than the hot spots further north (see Figure 24 and Figure 44). In contrast to the grassland growth induced from the spatial shift in settlement and agricultural production, this greening trend may rather be caused by climate change and higher temperatures, which is especially pronounced in central, eastern and northwestern locations of the Plateau [19]. Between 2005 and 2016 the average annual temperature over the Tibetan Plateau increased with 0.415°C per decade, as compared to 0.319 °C per decade observed over the last 50 years [43]. This significant warming could be responsible for the distinctive growth of grassland (Figure 35) especially from bare area (Figure 24).

The grassland trend suggests desertification or browning tendencies roughly in the first half of the study period and greening tendencies in the second half. From the transitions between grassland and bare area in Figure 42, the grassland growth seems to shift from being the less influential of the two transitions to the dominant one as of year 2001, where it passes the trend line for "grassland to bare area" (the peak of "bare area to grassland" in 1998 is not considered very reliable due to data issues discussed in subsection 4.2). This is also recognized in the total grassland area (Figure 35), and the pattern seems to concur with literature on vegetation greening, that suggest an overall greening trend for 1995-2004 and browning in 2005-2012

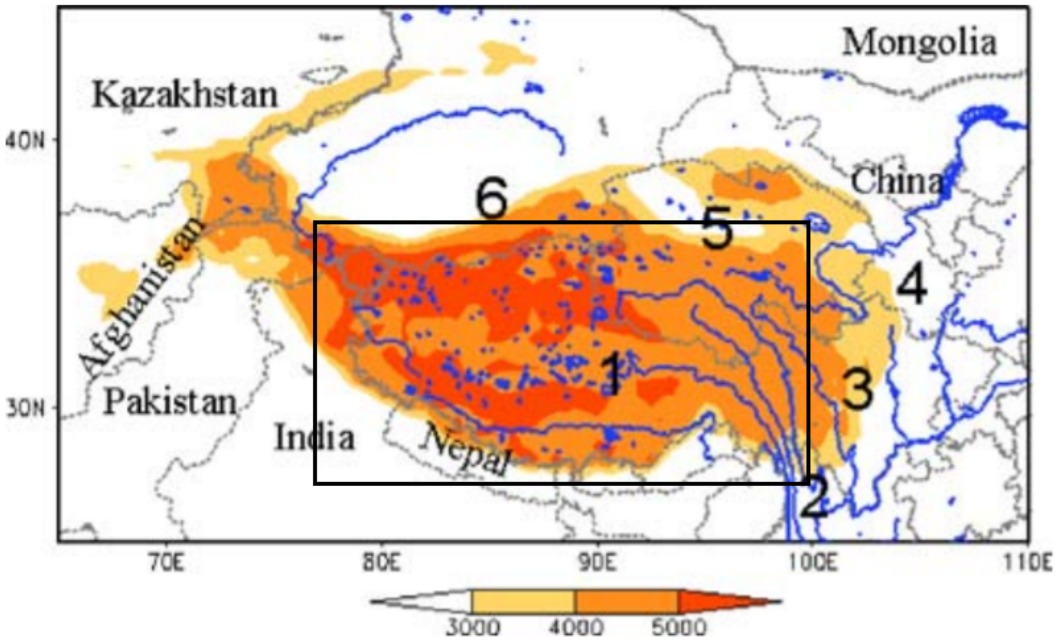

Figure 44. Elevation of the Tibetan Plateau and surrounding areas (orange shades). The area cut is marked approximately by the inner black rectangle, Chinese rivers and lakes are marked in blue and the locations that together make up the the Tibetan Plateau are the Tibet Autonomous Region (1) and parts of the provinces Yunnan (2), Sichuan (3), Gansu (4), Qinghai (4) and Xinjiang (6). Adapted from [10].

[44]. Increase in temperature and precipitation are both reasonable drivers for the greening tendencies [44]. Human activities related to agricultural practices and other types of land use may also affect vegetation growth [44]. However, considering the extensive spatial distribution of the transitions between bare area and grassland in addition to the lack of an apparent land use activity that would explain these interchanges, it seems plausible that the desertification and greening trends are caused by climate change.

Since the net increase in grassland area occurred at the expense of bare area, a consistent decline was seen for this LC class throughout the study period (Figure 39). However, significant grassland cover was also converted to bare area, mostly in other areas than where the grassland growth was manifested. This occurred especially at extreme high elevation (Figure 44, Figure 25). Changes from grassland to sparse vegetation (Figure 26) and from bare area to sparse vegetation (Figure 28) seem to be consistent with the geographical browning/desertification and greening pattern, respectively.

Considering the importance of the water sources at the Tibetan Plateau, the significant net increase in water area of 6.2 % deserves attention. 80 % of the 239 thousand hectares gained (net) in water bodies throughout the study period came from grassland. The gross change is mapped in Figure 29. There may be a series of possible explanations for this net gain of water area, and the most apparent drivers seem to be climate parameters such as temperature and precipitation. In recent decades (including the years of study i.e., 1992-2015) an increase has been observed both in temperature and precipitation at the Tibetan Plateau [43]. The latter, in combination with a measured decrease in (pan) evaporation [43], could explain the dispersion of water bodies. Higher temperatures may also lead to the retreat of glaciers, but where precipitation increase occur simultaneously this may compensate for the warming impact. A significant retreating effect of the glaciers located within the Tibetan Plateau has not yet been well documented [19].

4.2 Uncertainty

Limitations arising from choice of methods can be assigned two distinct origins:

1. Uncertainty in the collection and processing of satellite data, including classification methods
2. How the area cut represents the area of study

Regarding the first point, all satellite observations are associated with uncertainty. The ESA evaluates the overall accuracy of its CCI-LC maps to be about 71 %, but varying among the different LC classes and regions [15]. Some types of land cover could be mistakenly identified as something else, contributing to uncertainty from the classification process. The CCI-LC validation process also revealed surprisingly high accuracy values (around 90 %) among cropland classes (agriculture), despite that these are often associated with poor quality of the global LC data products available [15]. Of relevance to the classes considered in this thesis, the CCI-LC project furthermore reports relatively high accuracy among broadleaved evergreen forest, water bodies, bare areas and urban areas [15]. On the contrary, the use of CCI-LC data classified within the "Wetland" and "Sparse vegetation" category may be greater sources of uncertainty due to the lower accuracy values assigned these classes during validation [15]. Also, since wetland here is identified in some of the major LC transitions in Scandinavia in recent years, the uncertainty related to this class may be useful and important to understand better.

Although the original annual LC maps is given in LCCS labeled classes, the change detection is only performed at the accuracy level of IPCC LC categories, meaning that transitions between LC classes belonging to the same IPCC category are not captured in the CCI-LC maps [15]. However, this classification is useful and desired from a climate modelling perspective and makes the change detection more reliable in terms of avoiding false change detection among LC classes of similar definitions [15]. Also, for the purpose of this thesis, this approach is convenient since the focus is on the major LC classes and it is also based on the IPCC grouping. In situations where the objective is to study more specific LC classes (subcategories) e.g., the development of rainfed versus irrigated cropland, such a level of change detection does not have the required functionality. For this type of more detailed studies, and also for e.g. ecosystem and carbon flux accounting, a direct application of the UN LCCS may be preferred, or another methodological approach such as on-site field observations instead of or in addition to satellite images.

Furthermore, the change detection algorithm is based on 1 km observations, but delineated at 300 m to provide the higher resolution [15], meaning that only LC changes that can be identified from a distance of 1 km are detected. This may significantly influence the results for Scandinavia, because the CCI-LC map products are not able to capture changes happening along the coastlines [15].

Another potential source of error related to the change detection is that changes need to be confirmed over a period of two consecutive years for consistency [15]. Therefore, changes between 2014-2015 are limited to forests changes because these are the most easily detectable [15]. This limitation could explain why the LC changes for the first three years (1992-1994) and last two years (2014-2015) of the time series can hardly be observed. This seems to be the case for almost all of the LC classes (see total area charts and trend charts in subsection 3.3). Only changes in settlement (both regions), and to some degree forest (in Scandinavia), are clearly detected in the first and last years of the study and data period. This indicates that the quality of satellite data is highly dependent on the LC class and its change characteristics. Settlement changes may be more easily observed because these are of a more sudden character than e.g., the gradual and natural evolvement of grassland from abandoned agricultural land. This natural weakness of satellite data emphasizes the importance of high quality long-term data series for the proper detection of LUCC.

Sources of uncertainty may also differ among each of the satellite data sets used to create the CCI-LC maps. The AVHRR data, which is the foundation of the 1 km change detection from 1992 to 1999 [15], is reported to be of general lower quality compared to the other input data. Also, the change detection in 1994 is particularly uncertain due to lack of data for this specific year [15]. With these considerations in mind, the peaks of LC change observed in year 1994 and 1998 that seem to coincide in the two different regions (Figure 41, Figure 42) of no apparent reason may be explained by erroneous change detection from the AVHRR technology. If this is true, it has direct implications for the results and makes the LC changes

observed in 1992-1999 unreliable, or at least less credible.

With consideration to the second point, namely that the study area is made up of two regions created from "rectangular map cuts", it implies that the produced land cover matrices contain data also for surrounding land area as explained in subsection 2.2. To study LC changes happening in Norway and the Tibetan Plateau exclusively, a country/area datamask would need to be generated in order to separate LC data from neighboring countries/areas. In the case of Norway, the same applies for the separation of ocean water (and fjords) from inland water bodies which are the ones that are interesting to study in this context. Due to the data source being from satellite imagery, a distinction between the two is difficult on a color-basis, and require further modification of the raw data similar to that of a country mask. Such a datamask was not already available for the areas of study and would therefore need to be created, which is time consuming. For ease of computation, this analysis is conducted with the simpler map cut, that includes both ocean water and nearby LC from other countries than the intended regions of study. Clearly, this poses significant limitations to the interpretation of the results, firstly in terms of discussing to which degree the changes has occurred in the Tibetan Plateau/Norway, and secondly in relation to the water area and meaningful interpretation of this. The latter does not pose a major limitation in the analysis of LC change, because gain and loss of freshwater will still be detectable, as the ocean is not probable to have experienced big changes compared to inland water bodies.

Mapping LC transitions of interest as this thesis does, provides a useful foundation for qualitative and somewhat quantitative analysis of the spatial distribution of the individual gross LC transitions. Without a datamask separating the intended study area from the surroundings it is however difficult to quantify exactly how much of the change that has occurred within the area of study. Furthermore, it would also have been informative to display the total area of each LC class in a specific year on a map, but the resolution of the original data is too high for this purpose so the data would first need to be aggregated in a similar manner as the transitions provided for this thesis. Despite these limitations, the results can indicate general tendencies on LUCC within the area cut. Distributing the results from the LC change analysis on a map (e.g. in an visualization program such as IDV) reveals relevant hot spots and may contribute to a better understanding on the driving causes behind what is causing local and regional LC changes.

4.3 Conclusions and further work

Revisiting the research questions in subsubsection 1.2.1, these set out to identify and quantify recent LUCC. In light of this, this thesis has provided a better understanding of relevant recent changes and pointed out some possible explanations to these for the two regions of study. Both regions are affected by a significant and centralized growth in settlement and agricultural land. For the Tibetan Plateau this has had a special impact on its grasslands that are left to regenerate on previously cultivated lands. Furthermore, transitions among grassland, bare area and sparse vegetation indicate that a strong greening trend has occurred alongside with browning or desertification, but the hot spots of these two contrasting developments are mostly spatially separated. Greening also seems to be evident in northern Norway, by the recent growth from sparse vegetation to grassland. Results found in this thesis indicate that the greening trend is likely caused by changes in average temperature and rainfall in recent decades. Norway and neighboring countries has furthermore experienced a great loss of wetlands throughout the study period, where most of this is observed to have converted to forest area. As a LC type of major importance for ecosystem services and carbon fluxes, conservation efforts should be prioritized as a mitigation strategy for the Scandinavian countries.

The combination of the three analytical approaches has proven to be very useful in this thesis. The spatiotemporal transition analysis provided a good indication on which transitions are the major ones and should be prioritized for further study in each region. For Norway, this could be studies focusing on understanding the drivers behind the observed decline in wetland areas, and how this may be mitigated through policy prioritization. For the Tibetan Plateau, a continuous research focus on the complex land-atmospheric interactions is important in order to guide climate change mitigation action and conservation.

Understanding the reasons behind LC changes is crucial to determine where such conservation efforts should be prioritized. Additionally, the temporal analysis is especially important when dealing with long-term data

series from various sources, because it provides insight on the validity of the data. The results indicated a possible data weakness and source of uncertainty in the years covered by the AVHRR system.

In terms of general improvements of the analysis, the spatial accuracy of results in both regions could be improved by applying a datamask to explicitly study the area of interest. For Norway, it would be useful to combine the utilized data with a mechanism that separates freshwater bodies from ocean and fjords. If inland water bodies are to be studied in more detail, the CCI-LC Water Body Product (WBP) that separates inland waters from ocean at 150 m resolution [15], could be analysed separately to provide better estimates of water bodies along the coastlines which is especially limited in the annual LC maps.

Well aware of the limitations associated with satellite observations, the remote sensing community should focus on validation efforts to reduce uncertainty in the data. In this aspect, improvements in the CCI-LC product validation in terms of classification and change detection could be made by performing systematic comparisons with different LC datasets [13]. A more mixed sample based on various LC data sets may also provide overall better estimates of LC change [13] and in turn give better recommendations for land use policy. If possible, satellite observations should be validated by comparison with data collected from ground observation, which can provide for more detailed and local information and aid the understanding of interactions between human activity and land and atmosphere interactions. In the Tibetan Plateau there have been initiated several field experiment campaigns for this purpose [10]. In conjunction with satellite data, field work will also play an important role in providing the required inputs for the climate and ecosystem models that will be used in the MITISTRESS project [8].

Research that addresses the complex interconnected relationships between LUCC, climate and ecosystems in an integrated manner is a necessity for improving climate models [10]. Globally, there are few studies that systematically assess the interactions between human activities, natural phenomena and vegetation change over time [44]. A better understanding of the impacts from human activities on LC change may be achieved by using the satellite data in combination with more detailed land use data such as the Global Human Footprint Dataset, which contains integrated data on population density, built infrastructure and land use activities [44]. Such approaches may be able to address variable sustainability aspects, which will be important to effectively mitigate climate change currently and in the future.

References

[1] Jianguo Liu et al. "A Framework for Evaluating the Effects of Human Factors on Wildlife Habitat: the Case of Giant Pandas". In: *Conservation Biology* 13.6 (Dec. 1999), pp. 1360–1370. ISSN: 0888-8892. DOI: 10.1046/j.1523-1739.1999.98418.x. URL: http://doi.wiley.com/10.1046/j.1523-1739.1999.98418.x.

[2] Pete Smith et al. *Agriculture, Forestry and Other Land Use (AFOLU). In: Climate Change 2014: Mitigation of Climate Change. Contribution of Working Group III to the Fifth Assessment Report of the Intergovernmental Panel on Climate Change*. Tech. rep. 2014. URL: https://www.ipcc.ch/site/assets/uploads/2018/02/ipcc_wg3_ar5_chapter11.pdf.

[3] Edward A. G. Schuur et al. "Vulnerability of Permafrost Carbon to Climate Change: Implications for the Global Carbon Cycle". In: *BioScience* 58.8 (Sept. 2008), pp. 701–714. ISSN: 1525-3244. DOI: 10.1641/B580807. URL: https://academic.oup.com/bioscience/article/58/8/701/380621.

[4] Antonio Di Gregorio et al. *Classification Concepts. Land Cover Classification System. Software version 3*. Food and Agriculture Organization of the United Nations, 2016. ISBN: 9789251090176. URL: http://www.fao.org/3/a-i5232e.pdf.

[5] Haidong Li et al. "Human Impact on Vegetation Dynamics around Lhasa, Southern Tibetan Plateau, China". In: (2016). DOI: 10.3390/su8111146. URL: www.mdpi.com/journal/sustainability.

[6] Zaichun Zhu et al. "Greening of the Earth and its drivers". In: *Nature Climate Change* 6.8 (Aug. 2016), pp. 791–795. ISSN: 1758-678X. DOI: 10.1038/nclimate3004. URL: http://www.nature.com/articles/nclimate3004.

[7] Gregory Duveiller, Josh Hooker, and Alessandro Cescatti. "The mark of vegetation change on Earth's surface energy balance". In: *Nature Communications* 9.1 (Dec. 2018), p. 679. ISSN: 20411723. DOI: 10.1038/s41467-017-02810-8. URL: http://www.nature.com/articles/s41467-017-02810-8.

[8] NTNU. *Strategies to Mitigate Pressures on Terrestrial Ecosystems from Multiple Stressors (MITISTRESS)*. URL: https://www.ntnu.edu/ept/mitistress#/view/about.

[9] Chi Chen et al. "China and India lead in greening of the world through land-use management". In: *Nature Sustainability* 2.2 (Feb. 2019), pp. 122–129. ISSN: 2398-9629. DOI: 10.1038/s41893-019-0220-7. URL: http://www.nature.com/articles/s41893-019-0220-7.

[10] Xuefeng Cui and Hans-F. Graf. "Recent land cover changes on the Tibetan Plateau: a review". In: *Climatic Change* 94.1-2 (May 2009), pp. 47–61. ISSN: 0165-0009. DOI: 10.1007/s10584-009-9556-8. URL: http://link.springer.com/10.1007/s10584-009-9556-8.

[11] Anders Bryn et al. "Land cover in Norway based on an area frame survey of vegetation types". In: *Norsk Geografisk Tidsskrift* 72.3 (2018), pp. 131–145. ISSN: 15025292. DOI: 10.1080/00291951.2018.1468356.

[12] Jiyuan Liu et al. "China's changing landscape during the 1990s: Large-scale land transformations estimated with satellite data". In: *Geophysical Research Letters* 32.2 (Jan. 2005), p. L02405. ISSN: 0094-8276. DOI: 10.1029/2004GL021649. URL: http://doi.wiley.com/10.1029/2004GL021649.

[13] Wei Li et al. "Gross and net land cover changes in the main plant functional types derived from the annual ESA CCI land cover maps (1992-2015)". In: *Earth Syst. Sci. Data* 10 (2018), pp. 219–234. DOI: 10.5194/essd-10-219-2018. URL: https://doi.org/10.5194/essd-10-219-2018.

[14] Xiaoxuan Liu et al. "Identifying patterns and hotspots of global land cover transitions using the ESA CCI Land Cover dataset". In: *Remote Sensing Letters* 9.10 (Oct. 2018), pp. 972–981. ISSN: 2150-704X. DOI: 10.1080/2150704X.2018.1500070. URL: https://www.tandfonline.com/doi/full/10.1080/2150704X.2018.1500070.

[15] ESA. *Land Cover CCI: Product User Guide Version 2.0*. 2017. URL: http://maps.elie.ucl.ac.be/CCI/viewer/download/ESACCI-LC-Ph2-PUGv2_2.0.pdf.

[16] Goran Georgievski and Stefan Hagemann. "Characterizing uncertainties in the ESA-CCI land cover map of the epoch 2010 and their impacts on MPI-ESM climate simulations". In: *Theoretical and Applied Climatology* (Nov. 2018), pp. 1–17. ISSN: 0177-798X. DOI: 10.1007/s00704-018-2675-2. URL: http://link.springer.com/10.1007/s00704-018-2675-2.

[17] Haidong Li et al. "Elevation-Dependent Vegetation Greening of the Yarlung Zangbo River Basin in the Southern Tibetan Plateau, 1999–2013". In: *Remote Sensing* 7.12 (Dec. 2015), pp. 16672–16687. ISSN: 2072-4292. DOI: 10.3390/rs71215844. URL: http://www.mdpi.com/2072-4292/7/12/15844.

[18] Huai Chen et al. “The impacts of climate change and human activities on biogeochemical cycles on the Qinghai-Tibetan Plateau”. In: *Global Change Biology* 19.10 (Oct. 2013), pp. 2940–2955. ISSN: 13541013. DOI: 10.1111/gcb.12277. URL: http://www.ncbi.nlm.nih.gov/pubmed/23744573%20http://doi.wiley.com/10.1111/gcb.12277.

[19] Xiaodong Liu and Baode Chen. “Climatic warming in the Tibetan Plateau during recent decades”. In: *International Journal of Climatology* 20.14 (Nov. 2000), pp. 1729–1742. ISSN: 0899-8418. DOI: 10.1002/1097-0088(20001130)20:14<1729::AID-JOC556>3.0.CO;2-Y. URL: http://doi.wiley.com/10.1002/1097-0088%2820001130%2920%3A14%3C1729%3A%3AAID-JOC556%3E3.0.CO%3B2-Y.

[20] Yan-Zhi Zhao et al. “Assessing the ecological security of the Tibetan plateau: Methodology and a case study for Lhaze County”. In: *Journal of Environmental Management* 80.2 (July 2006), pp. 120–131. DOI: 10.1016/J.JENVMAN.2005.08.019. URL: https://www.sciencedirect.com/science/article/pii/S0301479705002781.

[21] Tandong Yao et al. “Third Pole Environment (TPE)”. In: *Environmental Development* 3 (July 2012), pp. 52–64. ISSN: 2211-4645. DOI: 10.1016/J.ENVDEV.2012.04.002. URL: https://www.sciencedirect.com/science/article/pii/S2211464512000760#bib74.

[22] J. Marc Foggin. “Depopulating the Tibetan Grasslands”. In: *Mountain Research and Development* 28.1 (Feb. 2008), pp. 26–31. ISSN: 0276-4741. DOI: 10.1659/mrd.0972. URL: http://www.bioone.org/doi/10.1659/mrd.0972.

[23] SSB. *Statistisk årbok 2013, Tabell 19: Samlet areal, arealfordelinger og kystlinjens lengde, etter fylke. 2013*. 2013. URL: https://www.ssb.no/a/aarbok/tab/tab-019.html.

[24] Anders Bryn et al. “A high-resolution GIS null model of potential forest expansion following land use changes in Norway”. In: *Scandinavian Journal of Forest Research* 28.1 (2013), pp. 81–98. ISSN: 02827581. DOI: 10.1080/02827581.2012.689005.

[25] Nærings- og handelsdepartementet. *Business and industry in Norway - The timber and pulp and paper industry*. June 2001. URL: https://www.regjeringen.no/no/dokumenter/Business-and-industry-in-Norway---The-timber-and-pulp-and-paper-industry/id419353/.

[26] Norwegian Ministry of Agriculture. *Norwegian Forests: Policy and Resources*. Tech. rep. URL: https://www.regjeringen.no/globalassets/kilde/ld/bro/2003/0001/ddd/pdfv/177177-norw_forests-brosj-eng.pdf.

[27] Urban Gunnarsson and Michael Löfroth. *The Swedish Wetland Survey – Compiled Excerpts From The National Final Report ISBN 978-91-620-6618-5*. Tech. rep. URL: www.naturvardsverket.se.

[28] *Norways Fifth National Report to the Convention on Biological Diversity*. Tech. rep. URL: https://www.cbd.int/doc/world/no/no-nr-05-en.pdf.

[29] Line Rochefort and Elve Lode. “Restoration of Degraded Boreal Peatlands”. In: *Boreal Peatland Ecosystems*. Springer Berlin Heidelberg, 2006, pp. 381–423. DOI: 10.1007/978-3-540-31913-9{_}17. URL: http://link.springer.com/10.1007/978-3-540-31913-9_17.

[30] W.J Fjellstad and W.E Dramstad. “Patterns of change in two contrasting Norwegian agricultural landscapes”. In: *Landscape and Urban Planning* 45.4 (Dec. 1999), pp. 177–191. ISSN: 0169-2046. DOI: 10.1016/S0169-2046(99)00055-9. URL: https://www.sciencedirect.com/science/article/pii/S0169204699000559.

[31] Lars Østbye Hemsing and Anders Bryn. “Three methods for modelling potential natural vegetation (PNV) compared: A methodological case study from south-central Norway”. In: *Norsk Geografisk Tidsskrift - Norwegian Journal of Geography* 66.1 (Feb. 2012), pp. 11–29. ISSN: 0029-1951. DOI: 10.1080/00291951.2011.644321. URL: http://www.tandfonline.com/doi/abs/10.1080/00291951.2011.644321.

[32] D MacDonald et al. “Agricultural abandonment in mountain areas of Europe: Environmental consequences and policy response”. In: *Journal of Environmental Management* 59.1 (May 2000), pp. 47–69. ISSN: 0301-4797. DOI: 10.1006/JEMA.1999.0335. URL: https://www.sciencedirect.com/science/article/pii/S0301479799903353.

[33] Birendra Bajracharya et al. “Understanding Land Cover Change Using a Harmonized Classification System in the Himalaya”. In: *Mountain Research and Development* 30.2 (May 2010), pp. 143–156. ISSN: 0276-4741. DOI: 10.1659/MRD-JOURNAL-D-09-00044.1. URL: http://www.bioone.org/doi/10.1659/MRD-JOURNAL-D-09-00044.1.

[34] Wei Li et al. "Major forest changes and land cover transitions based on plant functional types derived from the ESA CCI Land Cover product". In: *International Journal of Applied Earth Observation and Geoinformation* 47 (May 2016), pp. 30–39. ISSN: 1872826X. DOI: 10.1016/j.jag.2015.12.006. URL: https://www.sciencedirect.com/science/article/pii/S0303243415300714.

[35] *ESA/CCI viewer*. URL: http://maps.elie.ucl.ac.be/CCI/viewer/.

[36] Colorado) Unidata Program Center (of the University Corporation for Atmospheric Research (UCAR) Boulder. *Userguide: Unidata's Integrated Data Viewer version 5.6*. 2019. URL: https://www.unidata.ucar.edu/software/idv/docs/userguide/index.html.

[37] Justintools.com. *Convert Hectares to Soccer Fields*. URL: http://www.justintools.com/unit-conversion/area.php?k1=hectares&k2=soccer-fields&q=1550000.

[38] World Bank. *Population, total — Data*. URL: https://data.worldbank.org/indicator/SP.POP.TOTL.

[39] Anders Bryn. "Recent forest limit changes in south-east Norway: Effects of climate change or regrowth after abandoned utilisation?" In: *Norsk Geografisk Tidsskrift* 62.4 (2008), pp. 251–270. ISSN: 00291951. DOI: 10.1080/00291950802517551.

[40] *Skogbruk - Fylkesmannen i Trøndelag*. URL: https://www.fylkesmannen.no/Trondelag/Landbruk-og-mat/Skogbruk/.

[41] *Climate statistics – Yr*. URL: https://www.yr.no/place/Norway/climate.html#year.

[42] World Bank. *Managing Nepal's Urban Transition*. 2013. URL: https://www.worldbank.org/en/news/feature/2013/04/01/managing-nepals-urban-transition.

[43] Lingyi Tang et al. "Influences of climate change on area variation of Qinghai Lake on Qinghai-Tibetan Plateau since 1980s". In: *Scientific Reports* 8.1 (Dec. 2018), p. 7331. DOI: 10.1038/s41598-018-25683-3. URL: http://www.nature.com/articles/s41598-018-25683-3.

[44] Ya Liu et al. "Spatial and temporal patterns of global NDVI trends: Correlations with climate and human factors". In: *Remote Sensing* 7.10 (Oct. 2015), pp. 13233–13250. DOI: 10.3390/rs71013233.

Appendices

A CCI-LC products specifications

Table 6. Specifications on the available CCI-LC products [15]. The details of the LC maps used in this thesis is highlighted in yellow.

Product	Coverage		Resolution		Sensor	Projection	Format
	Spatial	Temporal	Spatial	Temporal			
MERIS SR time series	Global	2003-2012	300 m 1000 m	7-day	MERIS FR MERIS RR	WGS 84	NetCDF
AVHRR SR time series	Global	1992-1999	1000 m	7-day	AVHRR	WGS 84	NetCDF
PROBA-V SR time series	Global	2014-2015 (and beyond)	300 m	7-day	PROBA-V	WGS 84	NetCDF
Annual LC maps	Global	1992-2015	300 m	1-year	MERIS FR/RR SPOT-VGT AVHRR PROBA-V	WGS 84	NetCDF & GeoTiff
NDVI LS seasonality	Global	1999-2012	1000 m	7-day	SPOT-VGT	WGS 84	NetCDF & GeoTiff
Water body	Global	2000-2012	150 m	13-year	ASAR WSM	WGS 84	NetCDF & GeoTiff

Table 7. Satellite data sources used to generate the global LC maps [15]

Global LC database	Reference period	Satellite data source
Baseline 10-year global LC map	2003-2012	• MERIS FR/RR global SR composites between 2003 and 2012
Global annual LC maps	1992-1999	• Baseline 10-year global LC map • AVHRR global SR composites between 1992 and 1999 for back-dating the baseline
	1999-2013	• Baseline 10-year global LC map • SPOT-VGT global SR composites between 1999 and 2013 for up and back-dating the baseline • MERIS FR global SR composites between 2003 and 2012 to delineate the identified changes at 300 m spatial resolution • PROBA-V global SR composites at 300 m for year 2013 to delineate the identified changes at 300 m spatial resolution
	2014-2015	• Baseline 10-year global LC map • PROBA-V global SR composites at 1 km for years 2014 and 2015 for up-dating the baseline • PROBA-V time series at 300 m for 2014 and 2015 to delineate the identified changes the LC map spatial resolution

B Additional area graphics

Yearly area data for every LC class is listed in Table 8, and the area charts (Figure 45 and Figure 46) illustrate the change in total area of each LC class (that is not included in the result section) over the years 1992-2015.

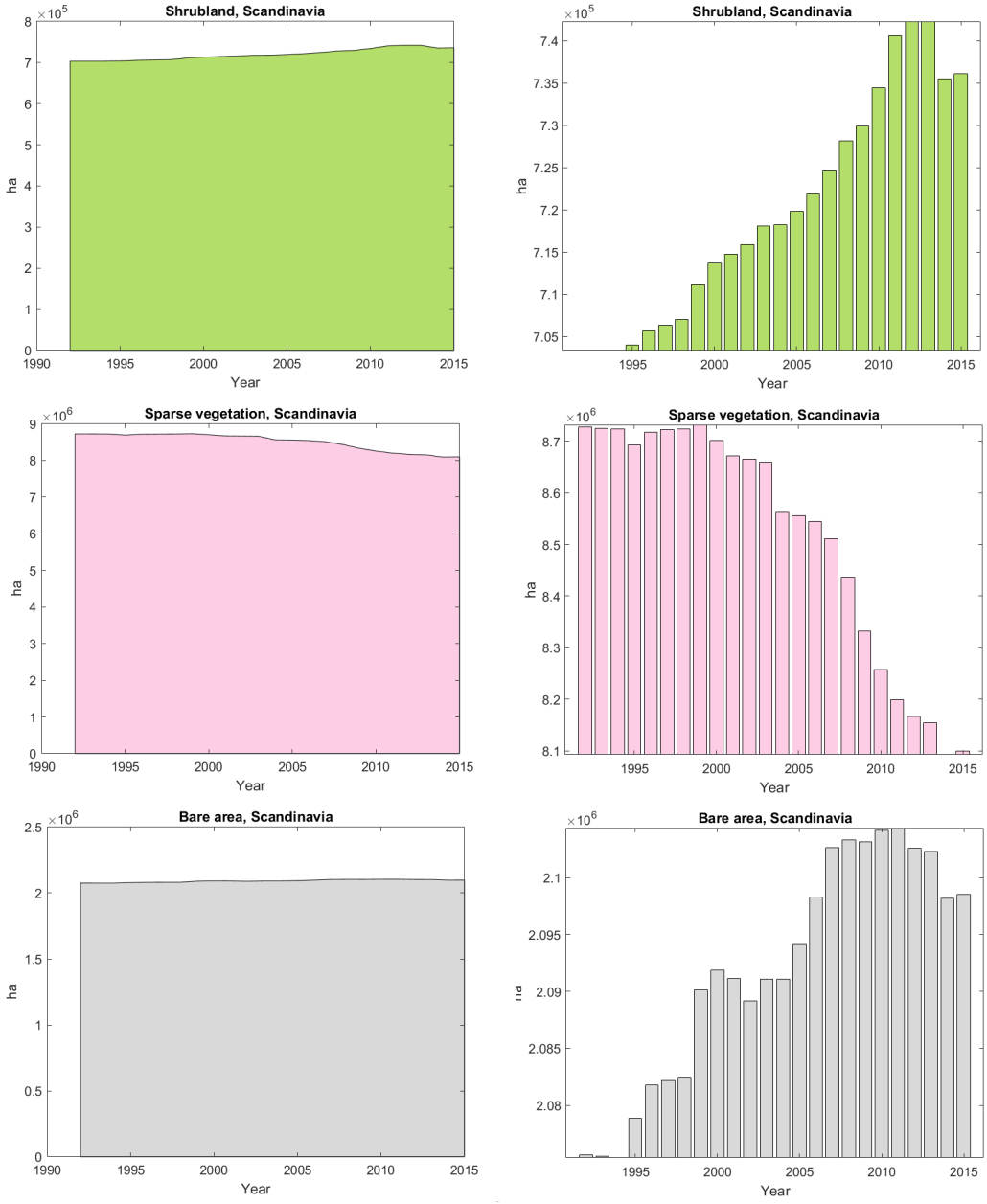

Figure 45. Total area (hectares) of shrubland, sparse vegetation and bare area in Scandinavia 1992-2015. The chart to the right displays the same area as the one to the left, but differs in the range of the vertical axis; it extends from the minimum value (instead of zero) to the maximum value of each category.

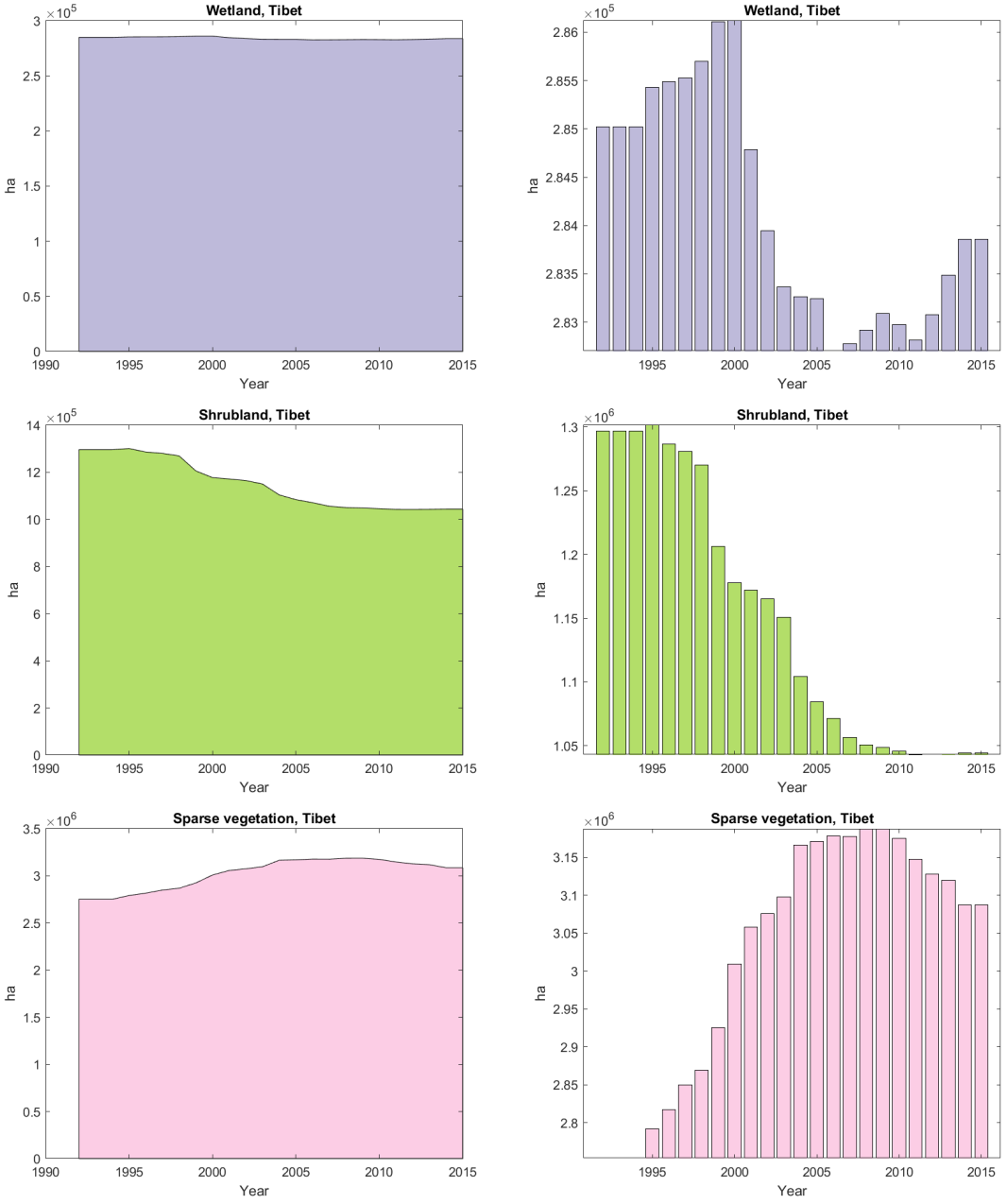

Figure 46. Total area (hectares) of wetland, shrubland and sparse vegetation in Tibet 1992-2015. The chart to the right displays the same area as the one to the left, but differs in the range of the vertical axis; it extends from the minimum value (instead of zero) to the maximum value of each category.

Table 8. Area (in million hectares) of each LC per year. Note that total area for water in Scandinavia not only counts inland water bodies but also ocean.

SCANDINAVIA

Year\LC class	Agriculture	Forest	Grassland	Wetland	Settlement	Shrubland	Sparse vegetation	Bare area	Water
1992	9.95	84.09	5.76	11.27	0.39	0.70	8.73	2.08	99.81
1993	9.95	84.09	5.76	11.27	0.40	0.70	8.73	2.08	99.81
1994	9.94	84.08	5.76	11.27	0.42	0.70	8.72	2.08	99.81
1995	9.99	84.22	5.78	11.13	0.43	0.70	8.69	2.08	99.76
1996	10.00	84.09	5.79	11.08	0.45	0.71	8.72	2.08	99.87
1997	10.01	84.04	5.80	11.06	0.47	0.71	8.72	2.08	99.89
1998	10.08	83.92	5.82	11.05	0.48	0.71	8.72	2.08	99.92
1999	10.30	84.03	5.91	10.74	0.50	0.71	8.73	2.09	99.77
2000	10.54	83.81	5.97	10.67	0.52	0.71	8.70	2.09	99.78
2001	10.57	83.97	6.00	10.46	0.54	0.71	8.67	2.09	99.76
2002	10.62	83.97	6.01	10.41	0.57	0.72	8.67	2.09	99.75
2003	10.66	83.92	6.02	10.37	0.59	0.72	8.66	2.09	99.76
2004	10.81	83.97	6.06	10.21	0.60	0.72	8.56	2.09	99.76
2005	10.89	83.90	6.07	10.19	0.62	0.72	8.56	2.09	99.75
2006	10.92	83.91	6.08	10.13	0.64	0.72	8.54	2.10	99.75
2007	10.96	84.03	6.08	10.01	0.65	0.72	8.51	2.10	99.72
2008	10.99	84.20	6.10	9.83	0.66	0.73	8.44	2.10	99.73
2009	11.07	84.42	6.13	9.62	0.67	0.73	8.33	2.10	99.71
2010	11.24	84.23	6.22	9.62	0.67	0.73	8.26	2.10	99.71
2011	11.39	84.00	6.31	9.65	0.68	0.74	8.20	2.10	99.72
2012	11.43	83.93	6.36	9.65	0.69	0.74	8.17	2.10	99.71
2013	11.44	83.93	6.37	9.64	0.69	0.74	8.15	2.10	99.71
2014	11.50	83.95	6.39	9.55	0.70	0.74	8.09	2.10	99.77
2015	11.50	83.94	6.39	9.55	0.70	0.74	8.10	2.10	99.77

TIBET

Year\LC class	Agriculture	Forest	Grassland	Wetland	Settlement	Shrubland	Sparse vegetation	Bare area	Water
1992	22.52	28.83	136.54	0.29	0.05	1.30	2.75	28.84	3.85
1993	22.52	28.83	136.54	0.29	0.05	1.30	2.75	28.84	3.85
1994	22.52	28.83	136.54	0.29	0.05	1.30	2.75	28.84	3.85
1995	22.44	28.91	136.27	0.29	0.05	1.30	2.79	29.07	3.83
1996	22.42	29.00	136.13	0.29	0.05	1.29	2.82	29.11	3.85
1997	22.45	28.99	136.02	0.29	0.05	1.28	2.85	29.17	3.86
1998	22.50	29.00	135.97	0.29	0.05	1.27	2.87	29.14	3.87
1999	22.80	28.86	136.15	0.29	0.06	1.21	2.93	28.81	3.86
2000	22.91	28.90	135.85	0.29	0.06	1.18	3.01	28.91	3.87
2001	22.81	28.89	135.86	0.28	0.07	1.17	3.06	28.90	3.92
2002	22.75	28.91	135.98	0.28	0.07	1.17	3.08	28.78	3.94
2003	22.70	28.96	136.00	0.28	0.08	1.15	3.10	28.73	3.96
2004	22.71	29.03	135.96	0.28	0.09	1.10	3.17	28.64	3.98
2005	22.68	29.06	136.03	0.28	0.09	1.08	3.17	28.57	3.99
2006	22.68	29.07	136.07	0.28	0.10	1.07	3.18	28.50	4.01
2007	22.65	29.10	136.19	0.28	0.10	1.06	3.18	28.38	4.02
2008	22.66	29.10	136.25	0.28	0.11	1.05	3.19	28.29	4.02
2009	22.67	29.10	136.30	0.28	0.11	1.05	3.19	28.23	4.03
2010	22.67	29.09	136.35	0.28	0.12	1.05	3.18	28.19	4.05
2011	22.66	29.09	136.49	0.28	0.12	1.04	3.15	28.08	4.05
2012	22.65	29.08	136.58	0.28	0.13	1.04	3.13	28.01	4.06
2013	22.63	29.07	136.62	0.28	0.14	1.04	3.12	28.00	4.07
2014	22.64	29.04	136.85	0.28	0.15	1.04	3.09	27.80	4.09
2015	22.63	29.04	136.85	0.28	0.15	1.04	3.09	27.80	4.09

C Computation

Table 9. 9x9 transition matrices, computed to generate the stacked plots, with a column for net change (gain or loss) added to the right of the transition matrix. As the red frames exemplify for wetland, area gains can be read off the columns and loss off the rows. Diagonal elements are naturally zero, but were included for easier computation and structure. Values are in hectares.

SCANDINAVIA

	Agriculture	Forest	Grassland	Wetland	Settlement	Shrubland	Sparse vegetation	Bare area	Water	Net gain/loss
Agriculture	0.00E+00	1.91E+05	7.99E+02	1.80E+03	1.11E+05	0.00E+00	3.27E+02	4.68E+01	4.25E+03	1.55E+06
Forest	1.77E+06	0.00E+00	3.43E+05	7.68E+05	1.61E+05	4.84E+04	1.79E+05	1.24E+04	4.80E+05	-1.55E+05
Grassland	6.96E+03	1.50E+05	0.00E+00	2.04E+03	2.56E+03	0.00E+00	5.91E+03	9.00E+01	4.47E+02	6.33E+05
Wetland	3.20E+04	2.38E+06	4.95E+04	0.00E+00	6.29E+03	7.85E+03	2.60E+04	1.01E+03	3.46E+04	-1.72E+06
Settlement	0.00E+00	0.00E+00	0.00E+00	0.00E+00	0.00E+00	0.00E+00	0.00E+00	0.00E+00	0.00E+00	3.14E+05
Shrubland	0.00E+00	2.53E+04	0.00E+00	1.39E+02	6.35E+01	0.00E+00	0.00E+00	0.00E+00	1.18E+01	3.27E+04
Sparse vegetation	2.10E+03	4.39E+05	3.76E+05	5.73E+03	2.35E+04	2.54E+02	0.00E+00	3.78E+04	3.00E+04	-6.28E+05
Bare area	0.00E+00	2.47E+03	2.29E+03	3.11E+01	1.38E+03	0.00E+00	3.75E+04	0.00E+00	2.84E+03	2.29E+04
Water	4.76E+04	4.22E+05	2.92E+04	3.81E+04	7.16E+03	1.69E+03	3.79E+04	1.81E+04	0.00E+00	-4.89E+04

Gross loss of wetland

Gross gain of wetland

TIBET

	Agriculture	Forest	Grassland	Wetland	Settlement	Shrubland	Sparse vegetation	Bare area	Water	Net gain/loss
Agriculture	0.00E+00	3.86E+05	5.12E+05	0.00E+00	8.21E+04	9.14E+02	1.86E+03	1.17E+04	3.83E+03	1.16E+05
Forest	5.22E+05	0.00E+00	7.27E+04	1.97E+03	4.76E+03	4.78E+04	1.57E+02	8.87E+02	5.27E+02	2.01E+05
Grassland	5.45E+05	1.81E+05	0.00E+00	1.60E+02	1.16E+04	7.51E+03	4.78E+05	1.34E+06	2.63E+05	3.05E+05
Wetland	0.00E+00	1.60E+02	0.00E+00	0.00E+00	2.45E+01	0.00E+00	0.00E+00	0.00E+00	5.52E+03	-1.16E+03
Settlement	0.00E+00	0.00E+00	0.00E+00	0.00E+00	0.00E+00	0.00E+00	0.00E+00	0.00E+00	0.00E+00	1.00E+05
Shrubland	2.59E+04	2.84E+05	1.11E+03	1.70E+01	4.58E+02	0.00E+00	8.90E+01	2.80E+02	2.36E+03	-2.50E+05
Sparse vegetation	4.10E+03	0.00E+00	3.28E+05	0.00E+00	3.95E+01	3.78E+02	0.00E+00	3.01E+04	4.11E+03	3.33E+05
Bare area	1.23E+04	0.00E+00	2.14E+06	1.88E+02	1.24E+03	5.81E+03	2.19E+05	0.00E+00	7.30E+04	-1.04E+06
Water	5.22E+03	1.94E+03	7.21E+04	2.20E+03	9.28E+01	1.31E+03	1.46E+03	2.87E+04	0.00E+00	2.39E+05